

1 Response: We thank the two reviewers and Dr. Harry ten Brink for thoughtful suggestions and
2 constructive criticism that have helped us improve our manuscript. Below we provide responses
3 to reviewer concerns and suggestions in blue font. All changes to the manuscript can be
4 identified in the version submitted using Track Changes.

5
6 **Anonymous Referee #1:**

7
8 In this very nice paper the authors attack constraints on aerosol-cloud interactions using aircraft
9 data off the California coast over many years of campaigns. Many studies use satellite
10 observations to do this and this study provides an important ground truth evaluation of this that is
11 needed by the field and gives additional information (for instance turbulence) that is not
12 available from space. This study shows the utility of sulfate in predicting variability in N_d , which
13 agrees with other studies. The data set in the study allows the authors to drill down into looking
14 at other species (sea salt, dust, organics) that have more elusive effects on N_d . My corrections
15 are mostly technical in nature.

16
17 L53 Adjustments may also include enhanced entrainment at cloud top (Ackerman et al., 2004).

18
19 Response: We added this effect and reference:

20
21 “For warm marine boundary layer (MBL) clouds at fixed liquid water, higher N_d values result in
22 (i) higher cloud albedo (thus cooling the Earth and counteracting the greenhouse effect)
23 (Twomey, 1977), (ii) delayed and/or reduced precipitation (Albrecht, 1989), and (iii) enhanced
24 entrainment at cloud top (Ackerman et al., 2004).”

25
26
27 L56 This is still the case in more recent reviews (Bellouin et al., 2020).

28
29 Response: Reference was added in that line:

30
31 “The complex interactions and feedback mechanisms between aerosols, meteorology, and clouds
32 leads to aerosol-cloud interactions as the largest source of uncertainty in climate models (IPCC,
33 2013; Bellouin et al., 2020).”

34
35
36 L181 In McCoy et al. 2018 the SS and DU was restricted to the submicron size bins from
37 MERRA2 and only hydrophilic BC/OC were used. All mass concentrations were taken at 910
38 hPa. Not critical to your study, but good to keep in mind to comparing to the better resolved data
39 from aircraft.

40
41 Response: A sentence was added at the end of the paragraph, which now reads:

42
43 “... A caveat to consider when comparing the findings of McCoy et al. (2018) to other aircraft
44 studies is that McCoy et al. (2018) used mass concentrations retrieved exclusively at the 910 hPa
45 model level (~ 915 m), and only considered mass concentrations pertaining to submicron SS/DU
46 and hydrophilic BC/OC.”

47 L351 While not essential to the analysis being performed here, one interesting possibility is for
48 the authors to train on the NiCE or FASE campaign and test the regression on the other wildfire-
49 affected campaign (reducing the risk of overfitting). One intriguing possibility is that not all fires
50 produce similar aerosol in terms of CCN activity and influence on CCN. Were the fires during
51 these campaigns in very different environments?

52
53 Response: We thank the reviewer for this insightful suggestion. Even though this study does not
54 make use of training, we do address the reviewer's suggestion by analyzing on the NiCE and
55 FASE campaigns separately. We find that FASE yields similar results to both campaigns
56 combined, but NiCE presents better correlations between all four species analyzed and N_d . Table
57 8 and a figure in the supplement were modified to include the new results.

58
59 Text was added to the end of Section 3.3.2 which reads:

60
61 "The NiCE (2015) and FASE (2016) campaigns were influenced by smoke originating from
62 different sources. NiCE was influenced by the Big Windy, Whiskey Complex, and Douglas
63 Complex forest fires near the California-Oregon border, with a transport time of approximately
64 two days to reach the base of aircraft operations in Marina and adjacent areas where most
65 samples were collected (Maudlin et al., 2015). In contrast, FASE was influenced by the
66 Soberanes fire approximately 30 km southwest of aircraft hangar (Braun et al., 2017). Hence,
67 analyzing each campaign separately may provide some insights into the sensitivity of N_d to
68 smoke from both different fuel types and with varying transport trajectories. NiCE fire data were
69 linked to timber, grass and shrub models whereas those from FASE were associated with
70 chaparral, tall grass, and timber (Braun et al., 2017; Mardi et al., 2018). The results are shown in
71 Table 8 and Figure S4. When comparing FASE to both campaigns combined, the prediction of
72 N_d using NSS-SO_4^{2-} , Na, Ox, and Fe is not improved, resulting in a ΔR^2_{adj} of -0.04, -0.04, 0.01,
73 and -0.03, respectively. However, when comparing NiCE to both campaigns combined, the
74 prediction of N_d using NSS-SO_4^{2-} , Na, Ox, and Fe is significantly improved, resulting in a ΔR^2_{adj}
75 of 0.14, 0.29, 0.18, and 0.13, respectively. The difference between NiCE and FASE could be
76 because different forest fires produce aerosols with varying aerosol chemical signatures and size
77 distributions, as studies in the region have shown (Ma et al., 2019; Mardi et al., 2019).
78 Alternatively, the difference could be due to the small sample size of NiCE (31 samples) as
79 compared to FASE (136 samples) (Table 1). Certainly more research, including larger datasets,
80 is warranted to investigate how different fuel types and plume aging times impact aerosol-cloud
81 interactions."

82
83
84 L431 The R^2 should always increase with more predictors, but R^2_{adj} won't necessarily?

85
86 Response: R^2_{adj} is useful when comparing two regressions that have a different number of
87 predictors. R^2 is corrected to produce R^2_{adj} using the number of predicting variables (P) and the
88 number of data points used in the regression (N) via the equation:

89
90
$$R^2_{adj} = 1 - (1 - R^2) (N-1) / (N-P-1).$$

91

92 For large values of N , R^2_{adj} is about equal to R^2 . For our data set, R^2 and R^2_{adj} differ by only
93 about 2%. Therefore, the asymptotic behavior in R^2_{adj} is also observed in R^2 , i.e., more predictors
94 do not necessarily increase R^2 (or R^2_{adj}). Despite the small difference between R^2 and R^2_{adj} , we
95 decided to use R^2_{adj} throughout the paper for the sake of rigor and consistency.

96
97 This issue is addressed by adding some text in Section 2.5, and in Section 3.2. The updated texts
98 now read:

99
100 “However, when comparing the performance of correlations between regressions using a
101 different number of predictor variables, it is necessary to use the adjusted coefficient of
102 determination (R^2_{adj}), which is subscripted to distinguish it from the ordinary R^2 , and is adjusted
103 by using the number of predictors (P) and the number of data points (N) via the formula $R^2_{adj} =$
104 $1 - (1 - R^2)(N - 1)/(N - P - 1)$ (Kahane, 2008). For a large number of data points, $R^2_{adj} \sim$
105 R^2 ; however, for the sake of rigor and consistency, R^2_{adj} is used instead of the ordinary R^2 , except
106 when reporting values from the literature.”

107
108 “It is also interesting to note how R^2_{adj} increases asymptotically to ~ 0.6 ; this further makes the
109 point that additional species do not necessarily improve predictability of N_d . The same
110 asymptotic behavior is also exhibited with R^2 , as R^2 and R^2_{adj} for these regressions differ by only
111 $\sim 2\%$.”

112
113
114 L413 The authors might find it helpful to make a predictor correlation matrix figure for this
115 section: https://seaborn.pydata.org/examples/many_pairwise_correlations.html

116
117 Response: We appreciate the suggestion and have added to the supplement a correlation matrix
118 which includes both the 9 predictor variables and the response variable (N_d). This matrix is used
119 to explain the possible multicollinearity causing some coefficients to have negative values. Text
120 was added to Section 3.2, and now reads:

121
122 “The physical reason as to why these species have negative coefficients when mixed with NH_4^+
123 is not clear; perhaps the reason is due to the mathematics of the regression and not physically
124 rooted, as the collinearity among three or more variables (called multicollinearity) can lead to
125 unexpected signs for predictor coefficients (Kahane, 2008). Furthermore, a correlation matrix
126 among the nine predicting species (Figure S2) shows a strong correlation for some pairs of
127 species ($\text{NH}_4^+ - \text{NO}_3^-$: $R^2_{adj} = 0.48$; $\text{NO}_3^- - \text{V}$: $R^2_{adj} = 0.49$) and moderate correlation for other pairs
128 ($\text{NH}_4^+ - \text{V}$: $R^2_{adj} = 0.27$; $\text{NO}_3^- - \text{Fe}$: $R^2_{adj} = 0.22$).”

129
130
131 L472 See note above regarding use of submicron SS from MERRA2 in the McCoy 2017/18
132 studies. One potential reason for this discrepancy is that the SS in MERRA2 is partially
133 indicative of dynamical mixing and turbulence, which the present study has information about. Is
134 it possible that the analysis approach in this study has disentangled this? L501 notes the strong
135 dependence of ocean-derived species on turbulence. Would it be possible to make a bivariate
136 plot of N_d as a function of SS and turbulence? This is done in Fig. 5, but going beyond binning
137 into high and low turbulence might be interesting to see.

138
139 Response: The reviewer makes an excellent point in suggesting that the discrepancy between the
140 value of the sea salt coefficient between McCoy et al. (2017, 2018) and the present study could
141 be due to the combined effects of turbulence and sea salt, and that the present study offers an
142 opportunity to separate these two effects. The reviewer's suggestions improved the quality of our
143 paper and we are grateful. A new figure was made and added to Section 3.3.1.

144
145 Text was added to the end of Section 3.3.1 which reads:

146
147 "For Na, there is a better correlation at high turbulent conditions than at smooth conditions (R^2_{adj}
148 = 0.26 and $R^2_{adj} = 0.09$ for high and low σ_w , respectively). This further strengthens the argument
149 that turbulence plays an important role in the vertical transport of sea salt (and other ocean
150 emissions) from the ocean surface to the cloud base. The present data set allows for deeper
151 analysis into the entangled effects of sea salt and turbulence on N_d . More specifically, aerosol
152 reanalysis products like those from MERRA-2 calculate the mass concentration of sea salt via
153 parameterizations that link wind speed to sea salt emissions (Gong et al., 2003; Randles et al.,
154 2017). Since wind speed affects turbulence, it follows that sea salt concentrations are not
155 independent from turbulence, as turbulence is used to calculate sea salt concentrations.
156 Subsequently, these sea salt concentrations are used to predict N_d (e.g., McCoy et al., 2017,
157 2018). The present study measured both sea salt (quantified by Na) and turbulence (quantified by
158 σ_w) and thus offers an opportunity to try to isolate the effects of both factors on N_d (Figure 6).
159 Two results emerge. First, more turbulence is correlated to more sea salt, which is consistent
160 with what the models predict (Randles et al., 2017). Second, at a fixed concentration of Na, N_d
161 does not vary significantly with σ_w , as evidenced by a weak change in color. However, at a fixed
162 value of σ_w , N_d does vary significantly with Na, as evidenced by the noticeable change in color.
163 Therefore, the independent measurement of both variables reveals that N_d is more sensitive to
164 changes in Na than to changes in σ_w . We caution that σ_w is not obtained from below the cloud,
165 but from within the cloud during sampling time (Figure S1)."

166
167 References:
168 Ackerman, A. S., Kirkpatrick, M. P., Stevens, D. E., and Toon, O. B.: The impact of
169 humidity above stratiform clouds on indirect aerosol climate forcing, *Nature*, 432, 1014-1017,
170 10.1038/nature03174, 2004.
171
172 Bellouin, N., Quaas, J., Gryspeerdt, E., Kinne, S., Stier, P., Watson-AR Parris, D., Boucher,
173 O., Carslaw, K. S., Christensen, M., Daniau, A. L., Dufresne, J. L., Feingold, G., Fiedler, S.,
174 Forster, P., Gettelman, A., Haywood, J. M., Lohmann, U., Malavelle, F., Mauritsen, T., McCoy,
175 D. T., Myhre, G., Mülmenstädt, J., Neubauer, D., Possner, A., Rugenstein, M., Sato, Y., Schulz,
176 M., Schwartz, S. E., Sourdeval, O., Storelvmo, T., Toll, V., Winker, D., and Stevens, B.:
177 Bounding Global Aerosol Radiative Forcing of Climate Change, *Rev Geophys*, 58,
178 10.1029/2019rg000660, 2020.

179

180 **Anonymous Referee #2:**

181
182 This paper describes the relationship between cloud droplet number concentration (N_d) and
183 cloud water composition using field measurements by aircraft flights off the California coast
184 over 4 multi-years campaigns. After the chemical analyses of the cloudwater samples, the data
185 were statistically analyzed to find the best correlations between chemical species and N_d . The
186 results highlight the importance of sulfate (both Total and non-sea-salt) in predicting N_d and its
187 variability, confirming findings already reported in previous studies. But the authors investigate
188 also the role of other chemical species (sea-salt, dust, organic matter) as well as of some other
189 factors (i.e., turbulence, cloud height, etc.). This is a very well-written paper that clearly
190 describes measurements, statistical approach and results which are also nicely compared to
191 previous findings. Even the possible drawbacks of the methodology and of the dataset are well
192 discussed by the Authors leaving no space for substantial criticism by my side. The results are of
193 interest for a large community investigating aerosol-cloud interaction from experimental and
194 modelling point of view and so the publication of this work is strongly recommended as it is.

195
196 I have only a question/comment (not influencing the final decision on this paper but maybe
197 interesting for future works): have the Authors any measurements/estimations of the acidity of
198 cloud water? pH has an important role in sulfate aerosol formation mechanism (Turnock et al.,
199 GRL, 2019), in the gas-particle partitioning of NH_4 and NO_3 and in solubility of metals (Pye et
200 al., ACP, 2020). Can the Authors comment about the possibility of testing pH as a
201 complementary predictor (maybe partially explaining the negative coefficients of some
202 regressions)?

203
204 Pye, H. O. T., Nenes, A., Alexander, B., Ault, A. P., Barth, M. C., Clegg, S. L., Collett Jr., J. L.,
205 Fahey, K. M., Hennigan, C. J., Herrmann, H., Kanakidou, M., Kelly, J. T., Ku, I.-T., McNeill, V.
206 F., Riemer, N., Schaefer, T., Shi, G., Tilgner, A., Walker, J. T., Wang, T., Weber, R., Xing, J.,
207 Zaveri, R. A., and Zuend, A.: The acidity of atmospheric particles and clouds, *Atmos. Chem.*
208 *Phys.*, 20, 4809–4888, <https://doi.org/10.5194/acp-20-4809-2020>, 2020.

209
210 Turnock, S. T., Mann, G. W., Woodhouse, M. T., Dalvi, M., O'Connor, F. M., Carslaw, K. S.,
211 and Spracklen, D. V.: The Impact of Changes in Cloud-Water pH on Aerosol Radiative Forcing,
212 *Geophys. Res. Lett.*, 46, 4039–4048, <https://doi.org/10.1029/2019GL082067>, 2019.

213
214 **Response:** We appreciate this thoughtful comment from the reviewer. To address the role of pH
215 on the ability to predict cloud droplet number concentration (N_d), H^+ (as quantified by pH) is
216 now included as a predicting species. Thus, the total number of species is now 80. However, pH
217 is poorly correlated to N_d , thus making it a bad predictor of N_d , and is dropped from the analysis
218 in Step 4 of the filtering algorithm (Figure 2). Therefore, the results of this study were not altered
219 by adding pH as a predicting species. The following parts of the manuscript have been modified
220 to reflect the inclusion of pH:

- 221
222 • Section 2.3 now includes a description of the pH analysis that reads:
223 “Cloud water sample acidity was quantified by measuring pH (the aqueous concentration of
224 hydrogen ions, H^+) using a Thermo Scientific Orion 9110DJWP Combination Semi-Micro
225 pH Electrode for E-PEACE, NiCE, and BOAS, and a Thermo Scientific Orion 8103BNUWP

226 Ross Ultra Semi-Micro pH probe for FASE. [...] This study uses air-equivalent
227 concentrations for all species with the exception of H^+ (pH) that uses aqueous concentration.”
228 • Table 2 and Figure 2 now include pH.
229 • Section 2.4 now includes a sentence highlighting that pH was removed from the analysis that
230 reads:
231 “Even though pH plays an important role in the partitioning of gases into particles and
232 droplets, in addition to influencing aqueous reactions in droplets (e.g., Pye et al., 2020), pH
233 was filtered out in Step 4 for being a poor predictor of N_d .”
234
235
236
237

238 **Comment from Dr. Harry ten Brink:**

239
240 I welcome a study in which the data on aerosol-cloud interaction is generalised. As a surprise I
241 notice that the parameterisation(s) as initiated 25 years ago like B&L still are central in
242 modelling.

243
244 Following are comments and questions

245
246 -I would have projected that a negative relation of N_d with Na would be seen because the few
247 large seasalt particles favourably compete with the smaller much more numerous sub-submicron
248 CCN composed of nSS (Steve Ghan). While in the remote ocean seasalt could increase CDNC it
249 seems highly unlikely this could occur off the coast in an area with sufficient small CCN as in
250 your case.

251
252 Response: We appreciate this insightful comment. Indeed, the effect of giant cloud condensation
253 nuclei (GCCN) like sea salt on cloud droplets and rain drops is of much interest to the aerosol-
254 cloud research community and deserved a better discussion. However, no conclusive results were
255 found in this study. A paragraph was added towards the end of Section 3.2 which reads:

256
257 “When considering a multi-species model to predict N_d , it is worthwhile to examine the coefficient
258 of sea salt. Even though it is well established that more CCN leads to more droplets, the effect of
259 giant CCN (GCCN), such as sea salt, is not as clear. Cloud microphysics studies suggest two
260 mechanisms by which more sea salt leads to less N_d : (1) The large size and highly hygroscopic
261 nature of sea salt causes these particles to activate into droplets before other smaller particles. This
262 reduces the amount of available water vapor and creates unfavorable conditions for smaller
263 particles to nucleate into droplets (e.g., Andreae & Rosenfeld, 2008). (2) GCCN nucleate into
264 larger droplets as compared to CCN, which in turn are more likely to collide and coalesce with
265 surrounding droplets. This combination of droplets creates larger but fewer droplets and ultimately
266 leads to the formation of rain drops and precipitation (e.g., Feingold et al., 1999, Jung et al., 2015).
267 Therefore, it is expected that the negative correlation between GCCN and N_d should translate into
268 a negative coefficient for Na (the sea salt tracer) in a multi-predictor regression equation. However,
269 this behavior was not observed in this study. A plausible explanation for this discrepancy is that
270 the effect of GCCN on N_d is highly dependent on conditions like LWC and N_d itself (e.g., Feingold
271 et al., 1999), and that this study did not capture the appropriate conditions to observe this effect.
272 However, McCoy et al. (2017) did observe a negative coefficient for sea salt and ascribed it to a
273 simulation artefact caused by the intimate link between sea salt generation and wind speed (i.e.,
274 turbulence). An attempt to isolate the effects of sea salt and turbulence on N_d is provided in Section
275 3.1.1.”

276
277 -line 459 e.f. the negative correlation with NO3 in case it is combined with ammonium seems to
278 me of quite some importance given the rather high values of the two as compared with sulphate.
279 What about a combination of sulphate and nitrate or rather nSS and nitrate, both deriving from
280 rather similar sources and possibly similar geographical location.

281
282 Response: This is a sensible comment because it is based on the desire to deduce physical
283 meaning from a mathematical result. However, we argue that the methodology used in this study

284 is limited and does not allow us to address such desire satisfactorily. The limitation is not in the
285 method of ordinary least squares (OLS), but rather in the data set fed into the OLS method. More
286 specifically, there are two limitations to the data set: (1) perhaps we did not define a strict
287 enough definition of collinearity when filtering species, and (2) we did not test for
288 multicollinearity in this study. Each limitation is described below.

- 289
290 (1) Say you have one independent (or response) variable, y , that you want to describe in terms of
291 two dependent (or predicting) variables, x_1 and x_2 , with a linear model of the form:

$$y = a x_1 + b x_2 + c$$

292
293
294
295 The ordinary least squares (OLS) method allows to find the coefficients (a , b , and c) which
296 best describe the data. However, the OLS method rests on the assumption that the predicting
297 variables x_1 and x_2 are not redundant. This redundancy is called “collinearity” and can be
298 assessed by applying the OLS method to x_1 and x_2 with an equation of the form:

$$x_1 = a x_2 + b$$

300
301
302 The predicting variables are said to be collinear if the regression yields a large correlation
303 coefficient (R). There is no universal definition of how large R needs to be for two predicting
304 variables to be considered collinear. When collinear predictors are fed into a model, there is
305 no guarantee that the sign or magnitude of the parameters will have any meaning. We
306 decided that two predictors were collinear if $R > 0.6$, but this could very well have been a
307 lenient criterion and could be a possible source of the unexpected sign and magnitude of the
308 NO_3^- , V, and Fe predictors.

- 309
310 (2) Now, say you have one response variable, y , that you want to describe in terms of **three**
311 predicting variables, x_1 , x_2 , and x_3 , with a linear model of the form:

$$y = a x_1 + b x_2 + c x_3 + d$$

312
313
314
315 The OLS method again allows to find the coefficients (a , b , c , and d), which best describe the
316 data. And again, the OLS method relies on the assumption that the predicting variables x_1 , x_2 ,
317 and x_3 are not redundant. To address this, the concept of “multicollinearity” is introduced,
318 which can be assessed by applying the OLS method to x_1 , x_2 , and x_3 with an equation of the
319 form:

$$x_1 = a x_2 + b x_3 + c$$

320
321
322
323 There is not a single metric to quantify multicollinearity, but for purposes of this rebuttal, we
324 shall use the adjusted correlation coefficient (R_{adj}). Similar to using two collinear predictors,
325 when multicollinear predictors are fed into a model, there is no guarantee that the sign or
326 magnitude of the parameters will have any meaning. **Furthermore, it is critical to point out**
327 **that just because the pairs x_1 - x_2 , x_1 - x_3 , and x_2 - x_3 are not collinear does not guarantee**
328 **that the x_1 - x_2 - x_3 set is not multicollinear.** Consider the fictitious data set below. If
329 collinearity and multicollinearity were defined as $R_{adj} > 0.5$, the pairs x_1 - x_2 , x_1 - x_3 and x_2 - x_3 are

330 all not collinear, but the x_1 - x_2 - x_3 set is multicollinear. Thus, it is likely that the coefficients for
 331 predictors x_1 , x_2 , and x_3 might lack meaning.
 332

x_1	x_2	x_3	Test for	Linear Equation	R_{adj}	
0.43	0.21	0.51	Collinearity between two variables	$x_1 = a x_2 + b$ or $x_2 = a x_1 + b$	0.4040	All pairs are not collinear
0.04	-0.18	0.55		$x_1 = a x_3 + b$ or $x_3 = a x_1 + b$	0.5953	
0.89	0.49	1.16		$x_2 = a x_3 + b$ or $x_3 = a x_2 + b$	-0.3481	
0.74	0.52	0.69				
0.64	-0.56	2.48				
0.65	-0.24	1.87				
-0.01	-0.53	1.03	Multi-collinearity between three variables	$x_1 = a x_2 + b x_3 + c$ or $x_1 = a x_3 + b x_2 + c$	0.9966	The x_1 - x_2 - x_3 set is multicollinear
0.24	-0.81	2.16		$x_2 = a x_1 + b x_3 + c$ or $x_2 = a x_3 + b x_1 + c$	0.9956	
0.21	0.97	-1.14		$x_3 = a x_1 + b x_2 + c$ or $x_3 = a x_2 + b x_1 + c$	0.9968	
0.4	-0.62	2.14				
0.75	-0.2	2.12				
0.78	0.63	0.53				
0.74	-0.6	2.97				
0.23	0.28	-0.08				
-0.54	-0.88	0.28				
0.86	0.99	0.27				
-0.44	-0.74	0.14				
0.7	0.2	1.28				
-0.51	0.29	-1.85				
-0.97	-0.66	-1.16				

333 The chemical composition of cloud water is a complex system, e.g., not all species can be
 334 attributed to their own individual source, and complex chemical reactions take place within
 335 droplets. When considering a complex system like the chemical composition of cloud water,
 336 it is reasonable to state that the more species are used to predict N_d , the higher the probability
 337 that the set of species being considered is multicollinear. We did not test for multicollinearity
 338 in this study. Therefore, it is not surprising that unexpected negative coefficients only appear
 339 when considering many (five) predictors; recall that at six predictors, all regressions become
 340 statistically insignificant. In other words, the unexpected sign and magnitude of the
 341 coefficients for NO_3^- , V, and Fe in a regression with five predictors is likely caused by
 342 multicollinearity among the predictors. This makes it difficult to gain insight into the
 343 physical-chemical processes involved.
 344

345
 346 It is helpful to keep in mind the intention we had when implementing the multivariable
 347 regression method in Section 3.2: qualitatively identify the “ingredient species” that comprise a
 348 decent set of N_d predictors, which we found to be a form of sulfate, an ocean emission tracer, and
 349 an organic tracer. Not testing for collinearity does not invalidate our finding. However, we
 350 appreciate Dr. Harry ten Brink’s comment and we added a paragraph at the end of Section 2.5
 351 that reads:
 352

353 “The correct functioning of the method of ordinary least squares requires that the set of n predicting
 354 variables in Equation 3 not be collinear. Multicollinearity is defined by a set of three or more
 355 predicting variables being collinear. Using a set of multicollinear predictors can produce unreliable
 356 estimates in both magnitude and sign of the coefficients (a_i) (Kahane, 2008). There is no universal
 357 marker for multicollinearity. Furthermore, multicollinearity can only be addressed when analyzing

358 all predictors together. For example, for a given set of three predictors (P_1 , P_2 , and P_3), even though
 359 the pairs P_1 - P_2 , P_1 - P_3 , and P_2 - P_3 are not collinear, there is no guarantee that the P_1 - P_2 - P_3 set is not
 360 multicollinear. When considering a complex system such as the chemical composition of cloud
 361 water, it is reasonable to assume that as more species are used to predict N_d , the higher the
 362 probability that the set of species is multicollinear. We did not test for multicollinearity in this
 363 study; the consequences of not doing so are explored in Section 3.2.”

364
 365 And more discussion is provided in Section 3.2 that now reads:

366
 367 “In addition, multicollinearity will become more likely as more predictors as considered.
 368 Therefore, it is not surprising that unexpected negative coefficients only appear when
 369 considering many (five) predictors. Lastly, a correlation matrix among the nine predicting
 370 species (Figure S2) shows a strong correlation for some pairs of species (NH_4^+ - NO_3^- : $R^2_{adj} =$
 371 0.48; NO_3^- -V: $R^2_{adj} = 0.49$) and moderate correlation for other pairs (NH_4^+ -V: $R^2_{adj} = 0.27$; NO_3^- -
 372 Fe: $R^2_{adj} = 0.22$), thus strengthening the argument that the negative coefficients are due to
 373 mathematical multicollinearity and not a physical or chemical reason.”

374
 375
 376 -line 132 sampling was inland in continental clouds

377
 378 Response: This is a good observation but does not affect the final conclusions of this study. To
 379 avoid confusion, the word “continental” was added where appropriate in Section 1, which now
 380 reads:

381
 382 “Leaitch et al. (1986) sampled continental stratiform and cumuliform clouds over Ontario,
 383 Canada [...]. Leaitch et al. (1992) suggested that [...] for both continental stratiform and
 384 cumuliform clouds [...].”

385
 386 Furthermore, the word “continental” is also added to the Leaitch et al. (1992) entry in Table 4.

387
 388
 389 -line 491. “...and it is worth noting that only five of our 385 samples are considered low
 390 turbulence according to the criterion of Leaitch et al.”. This contradicts the later conclusion that
 391 the data can be translated to the NE-coast situation. There should at least some discussion on the
 392 absence of stratus-like clouds in your region.

393
 394 Response: This comment contains several interesting points, please consider the following
 395 arguments:

396
 397 (1) Leaitch et al. (1996) (abbreviated as L96 in this answer) encountered a certain range of
 398 turbulence conditions and we encountered a different range of turbulence conditions, as seen
 399 in the table below.

	Leaitch et al. (1996)	This study
Number of samples	24	385
Range of turbulence	0.07—0.81 m s ⁻¹	0.10—0.51 m s ⁻¹
33 rd percentile, i.e., “smooth” conditions	0.17 m s ⁻¹	0.27 m s ⁻¹

66 th percentile, i.e., “turbulent” conditions	0.23 m s ⁻¹	0.32 m s ⁻¹
Number (percentage) of smooth samples	4 (17%)	5 (1%)

401
402
403
404
405
406
407
408
409
410
411
412
413
414
415
416
417
418
419
420
421
422
423
424
425
426
427
428
429
430
431
432
433
434
435
436
437
438
439
440
441
442
443
444

We believe that the small overlap between our percentage of “smooth” (i.e., low turbulence) samples (1%) versus L96’s (17%) does not invalidate our statement that the northeast Atlantic region resembles the northwest Pacific region. Rather, we believe that the small overlap can be explained from a statistical point of view, namely: (a) we have 16 times more data points than L96, and (b) we consider four campaigns/summers whereas L96 considers only one.

We found inspiration in L96’s approach to use a distribution of turbulence measurements to statistically define turbulent and smooth conditions in terms of the 33rd and 66th percentile, respectively. Naturally, considering more data points will change the shape of the distribution and consequently also change the statistical definition of “smooth” and “turbulent”. We consider that no edits on the manuscript are required to address this concern.

(2) Even though we think that the critique to our claim that the northeast Atlantic region resembles the northwest Pacific region is not justified based on the overlap of turbulence conditions (argument 1), we do think there is value to this critique because in Section 3.1, we compare our results to Leaitch et al. (1992). As pointed out by Dr. Harry ten Brink in the previous comment, Leaitch et al. (1992) studied continental clouds, whereas, L96 studied marine clouds. To address this valid concern, we adjusted our wording in Section 3.1 from “... suggestive of commonality between two **ocean** regions ...” to “... suggestive of commonality between two **coastal** regions ...”.

(3) We respectfully disagree that stratus-like clouds are absent in our study region, since stratocumulus clouds are a type of stratus clouds. To leave no doubt in the mind of the reader on the abundance of stratocumulus/stratus-like clouds in the study region, Section 2.1 (which was renamed “Aircraft campaigns and study region”) now includes a line of text which reads:

“The persistent summertime stratocumulus cloud deck located off the California coast offers the ideal natural laboratory to study aerosol-cloud-precipitation-meteorology interactions (Russell et al., 2013; Sorooshian et al., 2018).”

1006. first entry in the table: a common error made in citing this reference, though not expected in this paper on cloud-water sulphate: the unit in the Leaitch et al. paper of 1992 is cw-sulphate in nequivalents/m³.

Response: This is a good point. A footnote on Table 4 mentions the different units of the Leaitch et al. (1992) paper. What is wished to be emphasized when comparing our study to the Leaitch et al. (1992) study is mainly the slope (a_1) for cloud water sulfate air-equivalent concentration. Fortunately, the value of the slope is not affected by the units of sulfate concentration, as shown in the box below. We consider that no edits on the manuscript are required to address this concern.

<p>Sulfate concentration (x) has units of $\mu\text{g m}^{-3}$. The slope m is given by:</p> $m = \frac{\log(y_2) - \log(y_1)}{\log(x_2) - \log(x_1)}$ $m = \frac{\log\left(\frac{y_2}{y_1}\right)}{\log\left(\frac{x_2}{x_1}\right)}$	<p>Sulfate concentration (x^*) has units of nEq m^{-3}, where x^* is proportional to x, i.e., $x^* = c x$. The slope (m^*) is given by:</p> $m^* = \frac{\log(y_2) - \log(y_1)}{\log(x_2^*) - \log(x_1^*)} = \frac{\log\left(\frac{y_2}{y_1}\right)}{\log\left(\frac{cx_2}{cx_1}\right)} = \frac{\log\left(\frac{y_2}{y_1}\right)}{\log\left(\frac{x_2}{x_1}\right)}$ $m^* = \frac{\log\left(\frac{y_2}{y_1}\right)}{\log\left(\frac{x_2}{x_1}\right)}$
$m = m^*$	

445
446 However, it is worth mentioning that Leaitch et al. (1992) used a log-log format, whereas Leaitch
447 et al. (1996) used a log-linear format. In Table 4, we show the Leaitch et al. (1992) study, which
448 has the same format (with exception of the units) as the other studies in Table 4; thus, no
449 modifications to the table are required.

450
451
452 Finally I really dearly miss a back-trajectory analysis of at least some typical flights or those with
453 high nSS / NO3 and Na.

454
455 Response: We appreciate the observation that including a back-trajectory analysis enriches a
456 paper. However, several previous papers that have analyzed the study region all converge on the
457 same conclusion: the air in the study region is influenced by air mass transport from the north
458 and northwest. To address this concern other readers could also have, a short paragraph was
459 added at the end of Section 2.1 (which was renamed to “Aircraft campaigns and study region”),
460 and reads:

461
462 “Previous studies have used back-trajectory analysis to show that air in the MBL in the study
463 region is predominantly influenced by air mass transport from the north and northwest (Schlosser
464 et al., 2020; Wang et al., 2016; Wonaschütz et al., 2013). Thus, the cloud water in this study was
465 influenced by a variety of local and long-range sources such as ship exhaust (Chen et al., 2012;
466 Coggon et al., 2012), biomass burning (Prabhakar et al., 2014; Mardi et al., 2018), ocean emissions
467 (Dadashazar et al., 2017; MacDonald et al., 2018), continental pollution (Ma et al., 2019; Wang et
468 al., 2016), and dust (Mardi et al., 2019; Wang et al., 2014).”

469
470

471 **On the Relationship Between Cloud Water Composition and Cloud Droplet Number**
472 **Concentration**

473
474 Alexander B. MacDonald¹, Ali Hossein Mardi¹, Hossein Dadashazar¹, Mojtaba Azadi Aghdam¹,
475 Ewan Crosbie^{2,3}, Hafliði H. Jonsson⁴, Richard C. Flagan⁵, John H. Seinfeld⁵, Armin
476 Sorooshian^{1,6*}

477
478 ¹Department of Chemical and Environmental Engineering, University of Arizona, Tucson, AZ,
479 USA

480 ²Science Systems and Applications, Inc., Hampton, VA, USA

481 ³NASA Langley Research Center, Hampton, VA, USA

482 ⁴Naval Postgraduate School, Monterey, CA, USA

483 ⁵Department of Chemical Engineering, California Institute of Technology, Pasadena, CA, USA

484 ⁶Department of Hydrology and Atmospheric Sciences, University of Arizona, Tucson, AZ, USA

485

486 *Corresponding author: armin@email.arizona.edu

487 **Abstract**

488 Aerosol-cloud interactions are the largest source of uncertainty in quantifying
489 anthropogenic radiative forcing. The large uncertainty is, in part, due to the difficulty of predicting
490 cloud microphysical parameters, such as the cloud droplet number concentration (N_d). Even though
491 rigorous first-principle approaches exist to calculate N_d , the cloud and aerosol research community
492 also relies on empirical approaches such as relating N_d to aerosol mass concentration. Here we
493 analyze relationships between N_d and cloud water chemical composition, in addition to the effect
494 of environmental factors on the degree of the relationships. Warm, marine, stratocumulus clouds
495 off the California coast were sampled throughout four summer campaigns between 2011 and 2016.
496 A total of 385 cloud water samples were collected and analyzed for 7980 chemical species. Single-
497 and multi-species log-log linear regressions were performed to predict N_d using chemical
498 composition. Single-species regressions reveal that the species that best predicts N_d is total sulfate
499 ($R^2_{adj} = 0.40$). Multi-species regressions reveal that adding more species does not necessarily
500 produce a better model, as six or more species yield regressions that are statistically insignificant.
501 A commonality among the multi-species regressions that produce the highest correlation with N_d
502 was that most included sulfate (either total or non-sea salt), an ocean emissions tracer (such as
503 sodium), and an organic tracer (such as oxalate). Binning the data according to turbulence, smoke
504 influence, and in-cloud height allowed examination of the effect of these environmental factors on
505 the composition- N_d correlation. Accounting for turbulence, quantified as the standard deviation of
506 vertical wind speed, showed that the correlation between N_d with both total sulfate and sodium
507 increased at higher turbulence conditions, consistent with turbulence promoting the mixing
508 between ocean surface and cloud base. Considering the influence of smoke significantly improved
509 the correlation with N_d for two biomass burning tracer species in the study region, specifically
510 oxalate and iron. When binning by in-cloud height, non-sea salt sulfate and sodium correlated best
511 with N_d at cloud top, whereas iron and oxalate correlate best with N_d at cloud base.

512
513
514
515

516 **1. Introduction**

517 To assess the degree to which humans have altered Earth's climate, it is necessary to
518 quantify the effect that particles in the air (i.e., aerosols) have on clouds. Some fraction of aerosols
519 (called cloud condensation nuclei, CCN) activate into cloud droplets, thus impacting the cloud
520 droplet number concentration (N_d). For warm marine boundary layer (MBL) clouds at fixed liquid
521 water, higher N_d values result in (i) higher cloud albedo (thus cooling the Earth and counteracting
522 the greenhouse effect) (Twomey, 1977), and (ii) delayed and/or reduced precipitation (Albrecht,
523 1989), and (iii) enhanced entrainment at cloud top (Ackerman et al., 2004). The complex
524 interactions and feedback mechanisms between aerosols, meteorology, and clouds leads to aerosol-
525 cloud interactions as the largest source of uncertainty in climate models (IPCC, 2013; Bellouin et
526 al., 2020).

527 It is indispensable to know the value of N_d , but this is a difficult parameter to accurately
528 simulate and retrieve (Fountoukis & Nenes, 2005). There is a need to improve N_d retrievals from
529 satellite remote sensors, which provide broad spatial and temporal coverage in contrast to surface
530 sites and airborne research flights. Currently, N_d retrievals are limited to inferred values based on
531 values of cloud optical depth, cloud droplet effective radius, and temperature, along with
532 assumptions such as vertical homogeneity of N_d and monotonic increases in liquid water content
533 at a constant fraction of its adiabatic value (Grosvenor et al., 2018). Ultimately, measurements are
534 needed to better inform climate models about the cloud droplet activation process and better
535 constraining N_d values. Current general circulation models (GCMs) calculate N_d using the
536 properties of aerosol particles in one of two ways (Ghan et al., 1997; Menon et al., 2002). First,
537 there is a rigorous approach that is based on physical principles that predicts N_d based on aerosol
538 properties and meteorological conditions (Abdul-Razzak & Ghan, 2000). Second, there is an
539 empirical approach that parameterizes N_d using either the number concentration of aerosols, N_a [#
540 cm^{-3}], the number concentration of CCN, N_{CCN} [# cm^{-3}], or the mass concentration of chemical
541 species that comprise the aerosols (Ghan et al., 1997).

542 The rigorous approach predicts N_d by considering aerosol properties (e.g., size distribution
543 and chemical composition), microphysical processes (e.g., the seeding of cloud droplets by
544 particles, droplet growth, and droplet evaporation), and meteorological parameters (e.g., relative
545 humidity and the vertical updraft velocity transporting aerosols to cloud base) (e.g., Chuang et al.,
546 1992; Chuang & Penner, 1995; Nenes & Seinfeld, 2003; Partridge et al., 2012). This method is
547 based on the physical principle that an aerosol particle needs to be a CCN in order to seed a cloud
548 droplet; consequently, the input for this approach is N_a , from which to calculate N_{CCN} , and
549 subsequently N_d . The requisite information for these calculations may not be readily available for
550 GCMs. A limitation is that the spatial resolution of a GCM may be too coarse to capture the small-
551 scale spatial variation of updraft velocity (Ghan et al., 2011; West et al., 2014).

552 The empirical parameterization approach of interest in the present study uses the mass
553 concentration of one or several chemical species and correlates it/them directly to N_{CCN} or N_d .
554 Aerosols containing the sulfate ion (SO_4^{2-}) have long been known to serve as effective CCN
555 (Andreae & Rosenfeld, 2008; Charlson et al., 1992; Lance et al., 2009; Medina et al., 2007). Sulfate
556 is both contained in sea salt and is a product of the oxidation of gaseous sulfur dioxide (SO_2) (Hegg
557 et al., 1981; Quinn et al., 2017), so it is customary to isolate the anthropogenic contribution to total
558 SO_4^{2-} by considering its non-sea salt fraction (NSS- SO_4^{2-}). Therefore, most studies choose either
559 total SO_4^{2-} (denoted hereafter as Tot- SO_4^{2-}) or NSS- SO_4^{2-} to predict N_{CCN} and N_d (e.g., Leaitch et
560 al., 1992; Novakov et al., 1994; Saxena & Menon, 1999). Using the mass concentration of SO_4^{2-}
561 or any other chemical species to predict N_d : (i) circumvents the complex intermediate

562 microphysical steps to go from an aerosol particle to a cloud droplet and implicitly accounts for
563 such meteorological variables like updraft velocity, (ii) is based on actual measurements, and (iii)
564 can be compared directly to the mass concentration of different species produced by aerosol
565 transport models (e.g., Boucher & Lohmann, 1995; Chen & Penner, 2005). The limitations of using
566 an empirical parameterization are: (i) assuming a mass size distribution of the aerosols, (ii)
567 assuming that one or a few chemical species are responsible for all CCN, and (iii) uncertainty in
568 generalizing field data from one region (or a few regions) under specific conditions to the entire
569 globe for all conditions (Pringle et al., 2009). Despite these drawbacks, empirical correlations of
570 N_d and the mass concentration of different species are valuable. For example, of the 20 studies
571 addressing the cloud albedo effect considered in the IPCC Fourth Assessment Report (IPCC,
572 2007), half relied on empirical relationships to calculate N_d (Pringle et al., 2009).

573 Several studies have developed empirical correlations between N_{CCN} and the mass
574 concentration of SO_4^{2-} (e.g., Adams & Seinfeld, 2003; Hegg et al., 1993; Matsumoto et al., 1997).
575 However, the present objective is to focus on improving the prediction of N_d , not N_{CCN} , using the
576 mass concentration of SO_4^{2-} in addition to other species. A log-log relation is often used to correlate
577 the mass concentration of SO_4^{2-} to N_d with an equation of the form (e.g., Lowenthal et al., 2004):
578

$$579 \log(N_d) = a_0 + a_1 \log([\text{SO}_4^{2-}]) \quad (1)$$

580
581 where $[\text{SO}_4^{2-}]$ is the mass concentration in air [$\mu\text{g m}^{-3}$], and a_0 and a_1 are fitting parameters. A log-
582 log relation is chosen to accommodate large ranges in N_d and SO_4^{2-} and to reduce sensitivity of
583 results to the measurement accuracy of each individual parameter (Boucher & Lohmann, 1995).
584 The mass concentration of SO_4^{2-} can be obtained by analyzing either aerosol particles or cloud
585 water. When analyzing cloud water, the mass concentration of SO_4^{2-} dissolved in droplets [mg lit^{-1}]
586 is converted to the air-equivalent mass concentration [$\mu\text{g m}^{-3}$] by multiplying by the liquid water
587 content, LWC [g m^{-3}], in a cloud. The data used to create N_d - SO_4^{2-} empirical parameterizations are
588 typically derived from field campaigns, which differ in the region of analysis, sampling platforms
589 (aircraft or ground-based), measurement approach (e.g., in particle form or dissolved in cloud
590 water), and number of species analyzed. While the literature evaluating relationships between
591 cloud water composition and N_d is limited and largely from aircraft studies from more than a
592 decade ago, there is a growing number of datasets characterizing N_d and cloud water composition
593 that are of interest to continue this line of research. Examples include the recently completed
594 Cloud, Aerosol, and Monsoon Processes Philippines Experiment ([CAMP²Ex](#)) and the
595 North Atlantic Aerosols and Marine Ecosystems Study (NAAMES) (Behrenfeld et al., 2019), and the
596 current multi-year Aerosol Cloud meTeorology Interactions oVer the western ATlantic Experiment
597 (ACTIVATE) (Sorooshian et al., 2020). A summary of relevant past field work follows.

598 Leaitch et al. (1986) sampled [continental](#) stratiform and cumuliform clouds over Ontario,
599 Canada and showed a roughly linear relationship between N_d and SO_4^{2-} at low SO_4^{2-} concentrations
600 (below $\sim 5 \mu\text{g m}^{-3}$), and that the relationship leveled out at higher concentration (Novakov et al.,
601 1994). Leaitch et al. (1992) suggested that the low R^2 values for the linear regression between N_d
602 and SO_4^{2-} for both [continental](#) stratiform and cumuliform clouds (0.30 and 0.49, respectively)
603 stemmed from factors such as (i) other chemical species besides SO_4^{2-} , and variability in both (ii)
604 updraft wind speed and (iii) temperature. Pueschel et al. (1986) sampled clouds originating from
605 marine and continental air masses at a ground-based observatory at Whiteface Mountain, New
606 York. They found that emissions contributed strongly to SO_4^{2-} , and that a significant portion of
607 SO_4^{2-} -containing particles acted as CCN, and thus likely impacted N_d . Novakov et al. (1994)

608 sampled marine cumulus and stratocumulus clouds by El Yunque peak in Puerto Rico. Although
 609 they showed that N_{CCN} and SO_4^{2-} were highly correlated in both cumulus and stratocumulus clouds,
 610 they also found that N_d and SO_4^{2-} were weakly correlated for stratocumulus clouds, and not
 611 correlated for cumulus clouds. They attributed this difference to the effect of entrainment and
 612 mixing on cloud microphysics. Leaitch et al. (1996) sampled marine stratus clouds over the Gulf
 613 of Maine and the Bay of Fundy during the North Atlantic Regional Experiment (NARE) and
 614 showed that SO_4^{2-} was better correlated with N_d than nitrate (NO_3^-) (with an R^2 of 0.30 and 0.12,
 615 respectively). The R^2 between N_d and SO_4^{2-} increased when the data were stratified into bins of
 616 low and high turbulence, which was quantified as the standard deviation of vertical wind speed.
 617 They found that in situations with lower supersaturations, N_d was more influenced by turbulence
 618 than by either SO_4^{2-} or N_a . Menon & Saxena (1998) and Saxena & Menon (1999) sampled
 619 orographic clouds at a ground-based station at Mt. Mitchell, North Carolina. They found that SO_4^{2-}
 620 was the main contributor to cloud water acidity and a reliable tracer for anthropogenic pollution.
 621 Log-log regressions of SO_4^{2-} - N_d were binned according to the level of SO_4^{2-} , with not much
 622 difference observed between the different levels of pollution. Borys et al. (1998) and Lowenthal
 623 & Borys (2000) sampled warm marine stratiform clouds on the Island of Tenerife in the Canary
 624 Islands. They found that N_d was influenced by NSS - SO_4^{2-} , NO_3^- , pollution-derived trace elements,
 625 and elemental carbon (EC), signifying that species other than SO_4^{2-} influenced N_d . Despite the
 626 sampling site's proximity to African deserts, the mass concentration of crustal elements contained
 627 in dust was found to have little correlation with N_d . Also, the sea salt tracer sodium (Na^+) was
 628 found to have little correlation with N_d . Several studies (e.g., Boucher & Lohmann, 1995;
 629 Lowenthal et al., 2004; Menon et al., 2002; Van Dingenen et al., 1995) have combined field data,
 630 such as those mentioned above, in addition to other data sets, with the intention of producing a
 631 robust empirical prediction of N_d . Menon et al. (2002) provided a log-log multi-species prediction
 632 of N_d using SO_4^{2-} , organic matter, and sea salt. Organic carbon has been shown to increase N_d , as
 633 it affects the surface tension of cloud droplets (e.g., Facchini et al., 1999; Nenes et al., 2002).
 634 Additionally, nitric acid (HNO_3) has been linked with increased CCN activity and N_d based on
 635 modeling studies (Hegg, 2000; Kulmala et al., 1993; Xue & Feingold, 2004).

636 McCoy et al. (2017) used N_d data from the Moderate-Resolution Imaging
 637 Spectroradiometer (MODIS) satellite instead of in situ measurements. Second, aerosol mass
 638 concentration data were obtained from the Modern-Era Retrospective Analysis for Research and
 639 Applications version 2 (MERRA-2; Gelaro et al., 2017) reanalysis product and various aerosol
 640 transport models instead of in situ measurements. Third, the study region was more global in nature
 641 (albeit focusing on marine stratocumulus clouds) instead of a specific region. Fourth, since
 642 reanalysis data were used, a multi-species, multi-variable linear regression was performed:

$$643 \log(N_d) = a_0 + a_1 \log(SO_4^{2-}) + a_2 \log(SS) + a_3 \log(BC) + a_4 \log(OC) + a_5 \log(DU) \quad (2)$$

645 where SS is sea salt, BC is black carbon, OC is organic carbon, and DU is dust. McCoy et al.
 646 (2017) found that SO_4^{2-} was predominantly correlated with N_d , with sea salt, black carbon, organic
 647 carbon, and dust accounting for smaller contributions. A caveat to consider when comparing the
 648 findings of McCoy et al. (2018) to other aircraft studies is that McCoy et al. (2018) used mass
 649 concentrations retrieved exclusively at the 910 hPa model level (~ 915 m), and only considered
 650 mass concentrations pertaining to submicron SS/DU and hydrophilic BC/OC.

651 The field studies cited above still leave a series of unanswered questions that the current
 652 study aims to address: (i) How is the SO_4^{2-} - N_d relationship affected by vertical wind speed (Leaitch
 653

654 et al., 1992), turbulence (Leitch et al., 1996), and entrainment (Novakov et al., 1994)?; (ii) Why
655 do species such as sea salt and dust play such a minor role in influencing N_d , even when located
656 over the ocean and near a desert (Borys et al., 1998; McCoy et al., 2017, 2018)?; (iii) What is the
657 relationship between organic matter and N_d (McCoy et al., 2018; Nenes et al., 2002)?; and (iv) Can
658 the SO_4^{2-} - N_d correlation be improved by considering other chemical species (e.g., Hegg et al.,
659 1993; Leitch et al., 1992; Novakov & Penner, 1993)? The present study will examine these
660 questions using a data set comprised of in situ aircraft measurements collected off the California
661 coast during four field campaigns. In addition to meteorological and aerosol and cloud
662 microphysical measurements, a total of 385 cloud water samples were collected and analyzed for
663 7980 chemical species (ions and elements). Even though measurements were collected in only one
664 localized region, it is expected that the variety of conditions encountered over four summers,
665 together with the large number of chemical species analyzed, will help address the questions noted
666 above. The results of this work have implications for simulations and retrievals of N_d , in addition
667 to studies examining relationships between atmospheric chemistry and cloud microphysics.

668 2. Methodology

669 2.1. Aircraft campaigns and study region

670 This work reports results relevant to warm marine stratocumulus clouds off the California
671 coast based on field measurements from four field campaigns between 2011 and 2016, each during
672 the months of July and August. [The persistent summertime stratocumulus cloud deck located off
673 the California coast offers the ideal natural laboratory to study aerosol-cloud-precipitation-
674 meteorology interactions \(Russell et al., 2013; Sorooshian et al., 2018\).](#) For all field campaigns,
675 the Center for Interdisciplinary Remotely-Piloted Aircraft Studies (CIRPAS) Twin Otter was
676 deployed [out of Marina, California](#) with an almost identical instrumentation payload. The four
677 campaigns addressed in this study are: the Eastern Pacific Emitted Aerosol Cloud Experiment (E-
678 PEACE) (Russell et al., 2013; Wonaschütz et al., 2013), the Nucleation in California Experiment
679 (NiCE) (Crosbie et al., 2016; Maudlin et al., 2015), the Biological and Oceanic Atmospheric Study
680 (BOAS) (Wang et al., 2016), and the Fog and Stratocumulus Evolution (FASE) Experiment
681 (Dadashazar et al., 2017; MacDonald et al., 2018). Research flight information and tracks are
682 shown in Table 1 and Figure 1, respectively.

683 [Previous studies have used back-trajectory analysis to show that air in the MBL in the study
684 region is predominantly influenced by air mass transport from the north and northwest \(Schlosser
685 et al., 2020; Wang et al., 2016; Wonaschütz et al., 2013\). Thus, the cloud water in this study was
686 influenced by a variety of local and long-range sources such as ship exhaust \(Chen et al., 2012;
687 Coggon et al., 2012\), biomass burning \(Prabhakar et al., 2014; Mardi et al., 2018\), ocean emissions
688 \(Dadashazar et al., 2017; MacDonald et al., 2018\), continental pollution \(Ma et al., 2019; Wang et
689 al., 2016\), and dust \(Mardi et al., 2019; Wang et al., 2014\).](#)

690 2.2. Aircraft instrumentation

691 Aircraft instrumentation used in each campaign is described in detail in Sorooshian et al.
692 (2018). The relevant instrumentation used in the present study is as follows: aerosol size
693 distribution was measured using a Passive Cavity Aerosol Spectrometer Probe (PCASP; particle
694 diameter (D_p) \sim 0.1–2.6 μm ; Strapp et al., 1992); cloud droplet size distribution was measured
695 using a Forward Scattering Spectrometer Probe (FSSP; $D_p \sim$ 2–45 μm ; Gerber et al., 1999) and a
696 Cloud and Aerosol Spectrometer-Forward Scattering (CASF; $D_p \sim$ 1–61 μm ; Baumgardner et al.,
697 2001); rain drop size distribution was measured using a Cloud Imaging Probe (CIP; $D_p \sim$ 25–1600

700 μm ; Baumgardner et al., 2001); cloud liquid water content (LWC) was measured using a
701 Particulate Volume Monitor (PVM-100A; $D_p \sim 3\text{--}50 \mu\text{m}$; Gerber, 1994); three-dimensional wind
702 speeds were calculated by combining the pressure measurements from a five-hole radome gust
703 probe plumbed into the aircraft nose together with the aircraft velocity and altitude measurements
704 provided by the aircraft's Global Positioning System/Inertial Navigation System (GPS/INS).

705 Since LWC played a critical role in converting aqueous concentration to air-equivalent
706 concentration, the size range used to calculate N_d was bracketed to resemble the size range of the
707 PVM-100A. Therefore, N_d was defined in this study to be equivalent to the integration of the cloud
708 droplet size distribution between $D_p \sim 3\text{--}50 \mu\text{m}$, and was calculated using CASF (for E-PEACE)
709 and FSSP (NiCE, BOAS, and FASE). For the NiCE campaign, LWC measurements from the
710 PVM-100A instrument were unreliable; therefore, the LWC for NiCE was calculated instead using
711 FSSP data between $D_p \sim 3\text{--}50 \mu\text{m}$.

712

713 2.3. Cloud water collection and chemical analysis

714 A total of 385 cloud water samples were collected throughout the four campaigns using a
715 modified Mohnen slotted-rod collector, reported to collect droplets with $D_p \sim 5\text{--}35 \mu\text{m}$ (Hegg and
716 Hobbs, 1986). The cloud water was collected in polyethylene bottles and stored at $\sim 5^\circ\text{C}$ for
717 subsequent offline chemical analysis. The spatially-averaged location of each cloud water sample
718 is shown in Figure 1. Cloud water samples were chemically analyzed post-flight for ions using ion
719 chromatography (IC; Dionex ICS-2100) and for elements using inductively coupled plasma mass
720 spectrometry (ICP-MS; Agilent 7700 Series) for E-PEACE, BOAS, and NiCE or triple quadrupole
721 inductively coupled plasma mass spectrometry (ICP-QQQ; Agilent 8800 Series) for FASE. The
722 limit of detection (LOD) for each ion and element measured is shown in Table S1. The
723 concentration of non-sea salt (NSS) species was calculated using the relative abundance of a NSS
724 species to Na^+ in natural sea salt (Seinfeld & Pandis, 2016). Cloud water sample acidity was
725 quantified by measuring pH (the aqueous concentration of hydrogen ions, H^+) using a Thermo
726 Scientific Orion 9110DJWP Combination Semi-Micro pH Electrode for E-PEACE, NiCE, and
727 BOAS, and a Thermo Scientific Orion 8103BNUWP Ross Ultra Semi-Micro pH probe for FASE.
728 Aqueous concentrations (i.e., mass concentrations in the droplets [mg L^{-1}]) were converted to air-
729 equivalent concentrations (i.e., mass concentrations in the air [$\mu\text{g m}_{\text{air}}^{-3}$]) by multiplying aqueous
730 concentrations by the LWC and dividing by the mass density of water. This study uses air-
731 equivalent concentrations for all species with the exception of H^+ (pH) that uses aqueous
732 concentration.

733 A total of ~~7980~~ species (29 measured ionic species, 46 measured elemental species,
734 measured pH, and 4 NSS calculated species; Table 2) were considered in this study as an initial
735 pool of candidate species that could potentially be used to predict N_d . To facilitate the statistical
736 analysis in this study, the amount of chemical species were filtered from ~~7980~~ to only nine. The
737 steps used in this filtering process are summarized in the next section.

738

739 2.4. Filtering of chemical species

740 A focus in this study is to identify appropriate chemical species to use as predictors in a
741 linear regression model (addressed in Section 2.5). Good statistical practice (e.g., Freund et al.,
742 2010) recommends that two conditions must be met to produce a meaningful multivariable
743 regression: (1) the independent/predictor variables must not be redundant, i.e., they must not be
744 highly correlated among themselves (the property of high correlation is called collinearity), and
745 (2) each independent/predictor variable must have some correlation with the dependent/response

Formatted: Font: Italic

746 variable. There is no universal rule to define what is “highly” correlated, rather, it depends on the
747 nature of the data and the user’s judgement.

748 As using all 7980 species is impractical in terms of providing results that could be tested
749 and/or used by others, a filtering method was used to reduce the number of species. The filtering
750 method consisted of seven steps (Figure 2), the objective of which was to trim the total number of
751 species by an order of magnitude, leaving just a few that exhibited the following characteristics:
752 (1) the most data quality and quantity, (2) the least redundancy among themselves, (3) the highest
753 correlation with N_d , and (4) the most physical meaning. The decision to remove a species becomes
754 less objective and quantifiable towards the last steps in Figure 2. Each step is described below.

755 Step 1 removed species with less than 70% of data points. A species could have a low
756 amount of points because it was not analyzed in a field campaign or because the data quality from
757 the IC or ICP (ICP-MS or ICP-QQQ) was inadequate. Step 2 removed duplicate species that were
758 measured by both IC and ICP. Step 3 addressed Condition (2) by removing species that were
759 collinear (i.e., correlated among themselves). The criterion for a “high” correlation was to have a
760 correlation coefficient (R) > 0.6 and a p-value < 0.05 . For example, if a fixed number of five
761 species were all highly correlated between each other, then only one of the five species was kept,
762 and the rest were removed. This procedure is to consolidate “families” of three or more highly
763 correlated species to a single species and does not apply to pairs of highly consolidated species.
764 Step 4 addressed Condition (3) by removing species that were not correlated to N_d . The criterion
765 for a “low” correlation was to have a coefficient of determination (R^2) < 0.1 . Notice that Step 3
766 uses R whereas Step 4 uses R^2 ; this is because collinearity is determined not only by the value of
767 R but also the sign of R . Step 5 removes all but one organic species, oxalate (Ox), since this species
768 generally had the highest mass concentration of all the organic species and was considered to be
769 representative of all other organic species. Step 6 removed species that could not easily be
770 attributed to a physical process or chemical source. Step 7 added back into the analysis four species
771 that had been removed. This was done for the sake of having species that are known to have
772 relevant sources in the study region. Even though pH plays an important role in the partitioning of
773 gases into particles and droplets, in addition to influencing aqueous reactions in droplets (e.g., Pye
774 et al., 2020), pH was filtered out in Step 4 for being a poor predictor of N_d .

775 The nine species that survived the filtering scheme in Figure 2 are methanesulfonic acid
776 (MSA), ammonium (NH_4^+), NO_3^- , Ox, Tot-SO_4^{2-} , NSS-SO_4^{2-} , Fe, Na, and vanadium (V). These
777 species have known sources as follows. MSA: ocean biogenic (Sorooshian et al., 2009); NH_4^+ :
778 agriculture (Bauer et al., 2016), marine emissions (Bouwman et al., 1997), and wildfires (Reid
779 et al., 1998); NO_3^- and Ox: fire (Prabhakar et al., 2014; Maudlin et al., 2015); Tot-SO_4^{2-} : sea salt
780 (Seinfeld & Pandis, 2016), ocean biogenic (Charlson et al., 1987), and shipping (Coggon et al.,
781 2012), with NSS-SO_4^{2-} missing the sea salt contribution; Fe: dust (Jickells et al., 2005) and fire
782 (Maudlin et al., 2015); Na: sea salt (Seinfeld & Pandis, 2016); V: shipping (Wang et al., 2014).
783 Note that we retained both Tot-SO_4^{2-} and NSS-SO_4^{2-} ; this is to evaluate which correlates more with
784 N_d , as some studies have used Tot-SO_4^{2-} (e.g., Leaitch et al., 1992; Saxena & Menon, 1999),
785 whereas other have used NSS-SO_4^{2-} (Novakov et al., 1994; Boucher & Lohmann, 1995). Sections
786 3.1 and 3.2 will discuss these nine species, and the rest of Section 3 will focus on only four species
787 to be explained later. These species were analyzed by a multivariable regression model, which is
788 described in the next section.

789 2.5. Mathematical model

790

Formatted: Font: Italic

791 This study examines the relationship between cloud water mass concentration and N_d with
792 a multivariable linear model similar to that of McCoy et al. (2017, 2018):

$$793 \log(N_d) = a_0 + a_1 \log(M_1) + a_2 \log(M_2) + \dots + a_n \log(M_n) \quad (3)$$

794
795 where M_i is the air-equivalent mass concentration of species i [$\mu\text{g m}^{-3}$], a_i are fitting parameters,
796 and n is the number of species being considered. N_d is the dependent (or response) variable, and
797 M_1, M_2, \dots, M_n are the independent (or predictor) variables. The logarithmic forms of N_d and M_i
798 were correlated to account for a numerically large range of several orders of magnitude, and
799 because a log-log model is commonly used to correlate chemical composition to N_d (e.g., Boucher
800 & Lohmann, 1995; Menon et al., 2002; McCoy et al., 2017).

801 The Matlab software package was used to obtain multivariable linear regressions of the
802 form of Equation 3 using the method of ordinary least squares. The performance of a regression
803 was quantified using the coefficient of determination (R^2). However, when comparing the
804 performance of correlations between regressions using a different number of predictor variables,
805 it is necessary to use the adjusted coefficient of determination (R_{adj}^2 R_{adj}^2), which is subscripted to
806 distinguish it from the ordinary R^2 , and is adjusted by using the number of predictors (P) and the
807 number of data points (N) via the formula $R_{adj}^2 = 1 - (1 - R^2)(N - 1)/(N - P - 1)$ (Kahane,
808 2008). For a large number of data points, $R_{adj}^2 \sim R^2$; however, for the sake of rigor and consistency,
809 R_{adj}^2 is used instead of the ordinary R^2 , except when reporting values from the literature. The
810 statistical significance of correlations was quantified using the p-value obtained by doing a two-
811 tailed Student's t-test. Both R_{adj}^2 and p-values were given by the Matlab software after regression.
812 P-values were obtained for both the overall regression and each individual coefficient in the
813 regression, e.g., if a regression has three predictors, there are a total of five p-values: one for the
814 overall regression, three for the slope of each individual predicting variable, and one for the
815 intercept. In this study, a regression was considered to be statistically significant if all the p-values
816 were < 0.05 .

817
818 The correct functioning of the method of ordinary least squares requires that the set of n
819 predicting variables in Equation 3 not be collinear. Multicollinearity is defined by a set of three or
820 more predicting variables being collinear. Using a set of multicollinear predictors can produce
821 unreliable estimates in both magnitude and sign of the coefficients (a_i) (Kahane, 2008). There is
822 no universal marker for multicollinearity. Furthermore, multicollinearity can only be addressed
823 when analyzing all predictors together. For example, for a given set of three predictors ($P_1, P_2,$ and
824 P_3), even though the pairs P_1 - P_2 , P_1 - P_3 , and P_2 - P_3 are not collinear, there is no guarantee that the
825 P_1 - P_2 - P_3 set is not multicollinear. When considering a complex system such as the chemical
826 composition of cloud water, it is reasonable to assume that as more species are used to predict N_d ,
827 the higher the probability that the set of species is multicollinear. We did not test for
828 multicollinearity in this study; the consequences of not doing so are explored in Section 3.2.

829 2.6. Calculation of turbulence

830 Similar to Leitch et al. (1992) and Feingold et al. (1999), this study analyzes the effect of
831 turbulence on the ability to predict N_d . Turbulence was considered to be represented by the standard
832 deviation of the vertical wind speed (w) and is represented as σ_w . Also similar to Leitch et al.
833 (1992), this study classified conditions into turbulent and smooth regimes by considering the upper
834 and lower 333rd percentile of σ_w , respectively. Although the rigorous approach to calculate σ_w
835 uses the w from below the cloud (Twomey, 1959), this study used vertical wind speed data
836

837 collected throughout the sampling time (i.e., mostly inside the cloud, but also outside the cloud).
838 This was mainly because not all cloud water samples had an accompanying measurement of w
839 below the cloud. To justify using σ_w from the sampling time instead of below cloud σ_w , consider
840 Figure S1, which shows a representative time series of altitude, w , and σ_w for a cloud water sample
841 that was collected minutes before a below-cloud leg, which collected measurements of w . It can
842 be seen that the plots of w and σ_w are similar, and that an average σ_w calculated either way is still
843 in the bottom 33rd percentile. Therefore, for purposes of this study, we consider in-cloud turbulence
844 to reasonably approximate below-cloud turbulence.
845

846 2.7. Determination of smoke influence

847 One of the objectives of this study is to analyze the extent to which the presence of smoke
848 from wildfires affects the correlation between N_d and cloud water chemical composition. Thus, it
849 was important to identify cloud water samples that were influenced by smoke. Only the NiCE and
850 FASE campaigns were affected by wildfires. Mardi et al. (2018) identified vertical soundings in
851 the NiCE and FASE campaigns that were influenced by smoke by establishing smoke influence to
852 have a total aerosol number concentration ($N_d \geq 1000 \text{ cm}^{-3}$, as measured by the PCASP, in addition
853 to visual and olfactory detection of smoke by flight scientists. In this study, a cloud water sample
854 was considered to be influenced by smoke if it was collected during a research flight (RF) that
855 contains a vertical sounding identified by Mardi et al. (2018) to be influenced by smoke, even if
856 the cloud water sample was not necessarily collected near the sounding labelled as smoke-
857 influenced; this is a valid assumption based on the work of Mardi et al. (2019). The RFs considered
858 to be smoke-influenced in this study were NiCE RFs 16—23 and FASE RFs 3—11 and 13—
859 15.
860

861 3. Results and Discussion

862 With the refined list of nine physically-meaningful species from Section 2.4, we now
863 proceed to address the following questions: (1) What single species best predicts N_d ?; (2) How
864 many species are sufficient to predict N_d ?; (3) What is an effective combination of species to
865 predict N_d ?; and (4) How do several factors (i.e., turbulence, smoke-influence, and location along
866 cloud depth) affect the ability to reliably predict N_d ? These questions are addressed in order in
867 Sections 3.1—3.4.
868

869 3.1. Single-variable prediction of N_d

870 In this section, we analyze which of the nine species filtered out in Section 2.4 best predicts
871 N_d by itself without binning by external factors. These single-predictor regressions with no binning
872 are important, as they provide a baseline for subsequent sections in which multi-predictor
873 regressions and binning are used. Table 3 and Figure 3 display the ability of each of the nine
874 species to predict N_d . To have consistency with subsequent sections, R^2_{adj} is used instead of the
875 ordinary R^2 . The regression and the individual coefficients all were statistically significant.

876 Some previous studies predicted N_d using Tot-SO₄²⁻ (e.g., Leitch et al., 1992; Saxena &
877 Menon, 1999), whereas other studies used NSS-SO₄²⁻ (e.g., Novakov et al. 1994; Lowenthal et al.,
878 2004). We find that Tot-SO₄²⁻ is the best predictor, and that is better correlated to N_d ($R^2_{adj} = 0.40$)
879 than NSS-SO₄²⁻ ($R^2_{adj} = 0.29$). This is likely because Tot-SO₄²⁻ encompasses both sea salt particles
880 and non-sea salt particles, and thus gives a better approximation to the total number concentration
881 of CCN. In addition, Tot-SO₄²⁻ also had the largest slope ($a_1 = 0.32$), suggesting that N_d is more
882 sensitive to changes in Tot-SO₄²⁻ than other chemical species. Although HNO₃ has been observed

Formatted: Font: Italic

883 to increase N_d (e.g., Xue & Feingold, 2004), NO_3^- was found to be only moderately correlated with
884 N_d ($R^2_{adj} = 0.24$). The species with the lowest correlation was Fe ($R^2_{adj} = 0.05$). This low correlation
885 with N_d was also presented by other crustal metals ~~that~~-like Al ($R^2_{adj} = 0.01$) and Ti ($R^2_{adj} \sim 0$) (not
886 shown in Table 3). The low influence of crustal metals on N_d is consistent with the findings of
887 Lowenthal & Borys (2000). Some physical meaning can be extracted from the intercept of the
888 regression (a_0). If N_d is insensitive to the mass concentration of a species, then the slope (a_1) should
889 be zero; and N_d would be constant with a value of $N_d = 10^{a_0}$. These intercepts yield a range
890 of N_d of 108–412 cm^{-3} . These values are not unrealistic in clouds in this study region (e.g., Chen
891 et al., 2012; Lu et al., 2009; Wang et al., 2016).

892 To contrast with results of this work, Table 4 shows the regression parameters from other
893 studies when correlating N_d and SO_4^{2-} . For the sake of completeness, Table 4 shows regressions
894 that analyzed non-marine stratocumulus clouds, but in this comparison, we focus only on those
895 regressions that analyzed stratocumulus clouds. Our results (i.e., a_i coefficients and R^2) for Tot-
896 SO_4^{2-} reasonably match the results of Leitch et al. (1992), suggestive of commonality between
897 two ~~oceanic~~ coastal regions with differing meteorological conditions (i.e., northeast Pacific vs
898 northwest Atlantic) (Sorooshian et al., 2019). Our results for NSS- SO_4^{2-} also reasonably match
899 those of McCoy et al. (2017), which is noteworthy as McCoy et al. (2017) used satellite retrievals
900 and model aerosol concentrations for several stratocumulus decks around the world, whereas our
901 analysis used in situ data from a relatively small region. However, our NSS- SO_4^{2-} results differ
902 significantly from those of Novakov et al. (1994), which is understandable since the regression
903 presented by Novakov et al. (1994) has a p-value > 0.05 . Our data set does not achieve the degree
904 of correlation achieved by Lowenthal et al. (2004), who report the highest correlation for marine
905 clouds ($R^2 = 0.82$). The studies that analyzed stratocumulus clouds all report intercept values (a_0)
906 ~ 2.0 , which is consistent with our data.

907 908 3.2. Multi-variable prediction of N_d

909 When previous studies correlated N_d (or N_{CCN}) and the air-equivalent concentration of
910 chemical species and obtained a poor correlation, it was suggested that taking more chemical
911 species into consideration would improve the correlation (e.g., Leitch et al., 1992; Novakov et
912 al., 1994). In this this section we address the issue: “How many chemical species are necessary to
913 adequately predict N_d ?”. To answer this question, we use the nine filtered species from Section
914 2.4. Regressions of the form of Equation 3 are performed for every combination of species. The
915 number of predictors in the regressions are varied from one up to eight. The number of
916 combinations (C) that can be made with P predictors selected from S species is $C = S!/(S - P)!$.
917 Combinations that include Tot- SO_4^{2-} and NSS- SO_4^{2-} together are not considered, thus leaving a
918 total of 383 regressions.

919 Of the total 383 regression, only 67 were considered as statistically significant. Figure 4
920 shows the R^2_{adj} as a function of the number of predictors for both statistically significant and
921 insignificant regressions; the percentage of regressions that were statistically significant is shown
922 in Table S2. These results show that adding more predictors does not necessarily improve the
923 correlation, as all correlations that use six or more predictors are statistically insignificant. This
924 behavior is perhaps because the new species being added are redundant with respect to the species
925 that are already in the model (i.e., the new species is mathematically collinear with the old species).
926 It is also interesting to note how R^2_{adj} increases asymptotically to ~ 0.6 ; this further makes the point
927 that additional species do not necessarily improve predictability of N_d . The same asymptotic
928 behavior is also exhibited with R^2 , as R^2 and R^2_{adj} for these regressions differ by only $\sim 2\%$.

Formatted: Font: Italic

929 We examined the best regressions produced by a given number of predictors to explore the
930 factors that contribute to a respectable multivariable regression. Table 5 shows the three
931 statistically significant regressions that had the highest R^2_{adj} for a given number of predictors (one
932 to five). The predictors are ordered horizontally according to the value of their coefficient in order
933 to show qualitatively which species is more dominant in a regression. Eight of the nine chemical
934 species considered appear at least once in a regression, with the most common species being NH_4^+ ,
935 a form of SO_4^{2-} (total or non-sea salt), Na, Ox, and MSA. Sulfate (total or non-sea salt) appears in
936 12 of the 15 regressions, and in eight regressions it has the largest coefficient; this speaks to the
937 importance of SO_4^{2-} in predicting N_d . However, the appearance of Na and Ox and their non-
938 negligible slope also highlights the importance of considering them as well in a correlation; this is
939 clearly observed in the increase of R^2_{adj} when Na and Ox are added to a regression that contains
940 only NSS- SO_4^{2-} (Table 6). We believe that the ingredients that yield the higher R^2_{adj} in Table 6
941 are: (1) a form of SO_4^{2-} (such Tot- SO_4^{2-} or NSS- SO_4^{2-}), (2) a sea emissions tracer (such as Na), and
942 (3) an organic tracer (such as Ox). NH_4^+ was present in all the regressions; however, given that it
943 comes from diverse sources such as agriculture (ApSimon et al., 1987; Bauer et al., 2016), marine
944 emissions (Bouwman et al., 1997; Paulot et al., 2015), and wildfires (Maudlin et al., 2015; Reid et
945 al., 1998), it is difficult to assess if it contributes to the CCN budget or simply accompanies all
946 types of CCN. In other words, we suspect that NH_4^+ appears in all correlations because it generally
947 accompanies the three ingredients we propose make a good correlation: a form of SO_4^{2-} , a marine
948 emissions tracer, and an organic tracer.

949 It is of interest to note that combining a sea salt tracer (such as Na) with NSS- SO_4^{2-} in a
950 two-predictor model has about the same performance ($R^2_{adj} = 0.41$; Table 6) as a one-predictor
951 model using Tot- SO_4^{2-} ($R^2_{adj} = 0.40$; Table 3). We believe this is because Tot- SO_4^{2-} encompasses
952 the sea salt and the non-sea salt contribution to CCN about the same as the artificial mathematical
953 separation of the two. Also of interest is that when only looking at the statistically significant
954 regressions, only 17 regressions have species with negative coefficients (i.e., negative slopes). The
955 species with negative coefficients are NO_3^- , Fe, and V (not shown); more specifically, NO_3^- , Fe,
956 and V have negative coefficients when they are accompanied by NH_4^+ in the same regression. The
957 physical reason as to why these species have negative coefficients when mixed with NH_4^+ is not
958 clear; perhaps the reason is due to the mathematics of the regression and not physically rooted, as
959 multicollinearity can lead to unexpected ~~signs for predictor coefficients~~ (Kahane,
960 2008). magnitudes and signs for predictor coefficients (Kahane, 2008). In addition,
961 multicollinearity will become more likely as more predictors as considered. Therefore, it is not
962 surprising that unexpected negative coefficients only appear when considering many (five)
963 predictors. Lastly, a correlation matrix among the nine predicting species (Figure S2) shows a
964 strong correlation for some pairs of species (NH_4^+ - NO_3^- : $R^2_{adj} = 0.48$; NO_3^- -V: $R^2_{adj} = 0.49$) and
965 moderate correlation for other pairs (NH_4^+ -V: $R^2_{adj} = 0.27$; NO_3^- -Fe: $R^2_{adj} = 0.22$), thus
966 strengthening the argument that the negative coefficients are due to mathematical multicollinearity
967 and not a physical or chemical reason.

968 When considering a multi-species model to predict N_d , it is worthwhile to examine
969 the coefficient of sea salt. Even though it is well established that more CCN leads to more droplets,
970 the effect of giant CCN (GCCN), such as sea salt, is not as clear. Cloud microphysics studies
971 suggest two mechanisms by which more sea salt leads to less N_d : (1) The large size and highly
972 hygroscopic nature of sea salt causes these particles to activate into droplets before other smaller
973 particles. This reduces the amount of available water vapor and creates unfavorable conditions for
974 smaller particles to nucleate into droplets (e.g., Andreae & Rosenfeld, 2008). (2) GCCN nucleate

975 into larger droplets as compared to CCN, which in turn are more likely to collide and coalesce
976 with surrounding droplets. This combination of droplets creates larger but fewer droplets and
977 ultimately leads to the formation of rain drops and precipitation (e.g., Feingold et al., 1999, Jung
978 et al., 2015). Therefore, it is expected that the negative correlation between GCCN and N_d should
979 translate into a negative coefficient for Na (the sea salt tracer) in a multi-predictor regression
980 equation. However, this behavior was not observed in this study. A plausible explanation for this
981 discrepancy is that the effect of GCCN on N_d is highly dependent on conditions like LWC and N_d
982 itself (e.g., Feingold et al., 1999), and that this study did not capture the appropriate conditions to
983 observe this effect. However, McCoy et al. (2017) did observe a negative coefficient for sea salt
984 and ascribed it to a simulation artefact caused by the intimate link between sea salt generation and
985 wind speed (i.e., turbulence). An attempt to isolate the effects of sea salt and turbulence on N_d is
986 provided in Section 3.1.1.

987 Menon et al. (2002) and McCoy et al. (2017, 2018) are among the few studies that have
988 used multiple species to predict N_d (Table 7). Menon et al. (2002) used three species (sulfate,
989 organic matter, and sea salt). McCoy et al. (2017, 2018) used five species (sulfate, sea salt, black
990 carbon, organic carbon, and dust), but the 2017 study found the contribution of organic matter to
991 be negligible. McCoy et al. (2017) observed a negative coefficient for sea salt (i.e., more sea salt
992 leads to fewer cloud droplets); however, we do not observe the same trend in our results, as the
993 sea salt tracer (Na) always has a positive coefficient. In order to intercompare results with previous
994 studies, we selected species homologous to those of McCoy et al. (2017, 2018). We select NSS-
995 SO_4^{2-} for sulfate, Na for sea salt, oxalate for organic carbon, and Fe for dust. We did not measure
996 a species analogous to black carbon. The subsequent analysis examines only these four species
997 using single-predictor regressions.

999 3.3. Analysis of meteorological factors through binning

1000 Historically, the effect that meteorological factors have on the composition- N_d (or $-N_{CCN}$)
1001 empirical relationship has been examined by analyzing regressions after binning by turbulence
1002 (Leaitch et al., 1996), cloud type (Leaitch et al., 1992; Novakov & Penner, 1993), and region
1003 (McCoy et al., 2018). The following sections address the effects of turbulence, smoke influence,
1004 and location along cloud depth.

1006 3.3.1. Effect of turbulence

1007 Building upon the work of Leaitch et al. (1996), who studied how turbulence affects the
1008 correlation between Tot- SO_4^{2-} and N_d , this study extends that analysis to examine four additional
1009 species. Similar to Leaitch et al. (1996), this study quantified turbulence by the standard deviation
1010 of vertical wind speed (σ_w). Our range of σ_w was 0.10—0.51 m s^{-1} . Low turbulence was considered
1011 to be in the bottom 33rd percentile ($\leq 0.27 \text{ m s}^{-1}$), whereas high turbulence was taken to be values
1012 in the top 33rd percentile ($\geq 0.33 \text{ m s}^{-1}$). Leaitch et al. (1996) considered low and high turbulence
1013 to be $\sigma_w < 0.17 \text{ m s}^{-1}$ and $\sigma_w > 0.23 \text{ m s}^{-1}$, respectively, and it is worth noting that only five of our
1014 385 samples are considered low turbulence according to the criterion of Leaitch et al. (1996).
1015 Figure 5 and Table 8 show how R^2_{adj} depends on the predicting species and the turbulence regime;
1016 the scatterplots from which the R^2_{adj} are taken are shown in Figure S2S3.

1017 For NSS- SO_4^{2-} , there is no significant difference in R^2_{adj} when comparing all the points or
1018 by binning by σ_w . However, this is not the case for Tot- SO_4^{2-} , in which there is a large difference
1019 in the degree of correlation ($R^2_{adj} = 0.27$ and $R^2_{adj} = 0.55$ for low σ_w and high σ_w , respectively).
1020 This is in agreement with Leaitch et al. (1996), in which the correlation (albeit, not log-log)

Formatted: Indent: First line: 0.5"

1021 between Tot-SO₄²⁻ and N_d yielded an $R^2 = 0.53$ and $R^2 = 0.91$ for low and high σ_w , respectively.
1022 The difference in the behavior between Tot-SO₄²⁻ and NSS-SO₄²⁻ hints that the sea salt
1023 contributions to SO₄²⁻ (i.e., ocean-derived species) are the ones affected by turbulence, and hence
1024 explains the insensitivity NSS-SO₄²⁻ has to turbulence.

1025 ~~For Na, there is a better correlation at high turbulent conditions than at smooth conditions~~
1026 ~~($R^2_{adj} = 0.26$ and $R^2_{adj} = 0.09$ for high and low σ_w , respectively). This further strengthens the~~
1027 ~~argument that turbulence plays an important role in the vertical transport of sea salt (and other~~
1028 ~~ocean emissions) from the ocean surface to the cloud base.~~

1029 For Ox, the correlation improves at low turbulence ($R^2_{adj} = 0.30$), but not at high turbulence
1030 ($R^2_{adj} = 0.09$). We believe Ox behaves differently than Na because it does not necessarily just enter
1031 the cloud from below via updrafts, but rather it enters the cloud from above via entrainment of air
1032 from the free troposphere that can at times be enriched with organic species in the study region
1033 (Coggon et al., 2014; Crosbie et al., 2016; Hersey et al., 2009; Sorooshian et al., 2007).

1034 ~~For Fe, all turbulence scenarios yield a low correlation between Fe and N_d ,~~
1035 indicating that, overall, Fe is not a good predictor for N_d .

1036 ~~For Na, there is a better correlation at high turbulent conditions than at smooth conditions~~
1037 ~~($R^2_{adj} = 0.26$ and $R^2_{adj} = 0.09$ for high and low σ_w , respectively). This further strengthens the~~
1038 ~~argument that turbulence plays an important role in the vertical transport of sea salt (and other~~
1039 ~~ocean emissions) from the ocean surface to the cloud base. The present data set allows for deeper~~
1040 ~~analysis into the entangled effects of sea salt and turbulence on N_d . More specifically, aerosol~~
1041 ~~reanalysis products like those from MERRA-2 calculate the mass concentration of sea salt via~~
1042 ~~parameterizations that link wind speed to sea salt emissions (Gong et al., 2003; Randles et al.,~~
1043 ~~2017). Since wind speed affects turbulence, it follows that sea salt concentrations are not~~
1044 ~~independent from turbulence, as turbulence is used to calculate sea salt concentrations.~~
1045 ~~Subsequently, these sea salt concentrations are used to predict N_d (e.g., McCoy et al., 2017, 2018).~~
1046 ~~The present study measured both sea salt (quantified by Na) and turbulence (quantified by σ_w) and~~
1047 ~~thus offers an opportunity to try to isolate the effects of both factors on N_d (Figure 6). Two results~~
1048 ~~emerge. First, more turbulence is correlated to more sea salt, which is consistent with what the~~
1049 ~~models predict (Randles et al., 2017). Second, at a fixed concentration of Na, N_d does not vary~~
1050 ~~significantly with σ_w , as evidenced by a weak change in color. However, at a fixed value of σ_w , N_d~~
1051 ~~does vary significantly with Na, as evidenced by the noticeable change in color. Therefore, the~~
1052 ~~independent measurement of both variables reveals that N_d is more sensitive to changes in Na than~~
1053 ~~to changes in σ_w . We caution that σ_w is not obtained from below the cloud, but from within the~~
1054 ~~cloud during sampling time (Figure S1).~~

1055

1056 3.3.2. Effect of smoke influence

1057 The clouds in the study region are affected by the smoke from wildfires (e.g., Dadashazar
1058 et al., 2019; Maudlin et al., 2015; Schlosser et al., 2017). As mentioned in Section 2.7, Mardi et
1059 al. (2018) used the same data set as this study and identified research flights (RFs) that contained
1060 smoke-influenced cloud soundings, namely NiCE RFs 16—23 and FASE RFs 3—11 and 13—
1061 15. In this study, we considered that all cloud water samples collected during the aforementioned
1062 RFs were influenced by smoke. Furthermore, we did not distinguish if the smoke was above or
1063 below in the cloud; this is an important caveat, as cloud microphysical properties seem to depend
1064 on the surrounding smoke vertical profile (e.g., Diamond et al, 2018; Koch & Del Genio, 2010).
1065 The correlation between N_d and composition as a function of smoke influence is shown in Figure
1066 ~~67~~ and Table 8, and the scatterplots from which the R^2_{adj} are taken are shown in Figure ~~S3S4~~.

Formatted: Indent: First line: 0.5"

1067 Species that are produced during wildfires exhibited an improvement in R^2_{adj} when considering
1068 only the smoke-influenced cases. The opposite is true for species not produced during wildfires.
1069 More specifically, Ox and Fe showed an increase in correlation for smoke-influenced conditions
1070 ($R^2_{adj} = 0.42$ and $R^2_{adj} = 0.15$ for Ox and Fe, respectively) and a small decrease in for smoke-free
1071 conditions ($R^2_{adj} = 0.07$ and $R^2_{adj} = 0.04$ for Ox and Fe, respectively). This is most likely because
1072 Ox and Fe concentrations increase during wildfires (e.g., Maudlin et al., 2015) and thus contribute
1073 appreciably to the regional CCN during the summertime when wildfires are prevalent.

1074 NSS-SO₄²⁻ and Na showed a decrease in correlation for smoke-influenced conditions (R^2_{adj}
1075 = 0.22 and $R^2_{adj} = 0.17$ for NSS-SO₄²⁻ and Na, respectively), and an increase for smoke-free
1076 conditions ($R^2_{adj} = 0.36$ and $R^2_{adj} = 0.24$ for NSS-SO₄²⁻ and Na, respectively). We suspect this is
1077 because even though wildfires can produce NSS-SO₄²⁻ (e.g., Reid et al., 1998) and Na (e.g.,
1078 Hudson et al., 2004; Silva et al., 1999), these species are not produced as effectively as Ox or Fe.
1079 For example, Maudlin et al. (2015) measured aerosol mass concentration in the study region during
1080 both smoke-influenced and non-smoke-influenced conditions. They reported an increase in mass
1081 concentration for NSS-SO₄²⁻, Na, Ox, and Fe to be 30%, 120%, 220%, and 408%, respectively,
1082 for submicron particles, and -2%, -28%, 164%, and 97%, respectively, for supermicrometer
1083 particles. Consequently, Ox and Fe are produced more in wildfires in the study region than NSS-
1084 SO₄²⁻ and Na.

1085 The NiCE (2015) and FASE (2016) campaigns were influenced by smoke originating from
1086 different sources. NiCE was influenced by the Big Windy, Whiskey Complex, and Douglas
1087 Complex forest fires near the California-Oregon border, with a transport time of approximately
1088 two days to reach the base of aircraft operations in Marina and adjacent areas where most samples
1089 were collected (Maudlin et al., 2015). In contrast, FASE was influenced by the Soberanes fire
1090 approximately 30 km southwest of aircraft hangar (Braun et al., 2017). Hence, analyzing each
1091 campaign separately may provide some insights into the sensitivity of N_d to smoke from both
1092 different fuel types and with varying transport trajectories. NiCE fire data were linked to timber,
1093 grass and shrub models whereas those from FASE were associated with chaparral, tall grass, and
1094 timber (Braun et al., 2017; Mardi et al., 2018). The results are shown in Table 8 and Figure S4.
1095 When comparing FASE to both campaigns combined, the prediction of N_d using NSS-SO₄²⁻, Na,
1096 Ox, and Fe is not improved, resulting in a ΔR^2_{adj} of -0.04, -0.04, 0.01, and -0.03, respectively.
1097 However, when comparing NiCE to both campaigns combined, the prediction of N_d using NSS-
1098 SO₄²⁻, Na, Ox, and Fe is significantly improved, resulting in a ΔR^2_{adj} of 0.14, 0.29, 0.18, and 0.13,
1099 respectively. The difference between NiCE and FASE could be because different forest fires
1100 produce aerosols with varying aerosol chemical signatures and size distributions, as studies in the
1101 region have shown (Ma et al., 2019; Mardi et al., 2019). Alternatively, the difference could be due
1102 to the small sample size of NiCE (31 samples) as compared to FASE (136 samples) (Table 1).
1103 Certainly more research, including larger datasets, is warranted to investigate how different fuel
1104 types and plume aging times impact aerosol-cloud interactions.

1105 3.3.3. Effect of in-cloud height

1107 MacDonald et al. (2018) used the same data set as this study to show that the chemical
1108 composition of cloud water varies with height within a cloud. It is therefore reasonable that the
1109 N_d -chemical composition relationship also varies with in-cloud height. The correlation between N_d
1110 and composition as a dependence of in-cloud height is shown in Figure 78 and Table 8, and the
1111 scatterplots from which the R^2_{adj} are taken are shown in Figure S4S5.

1112 Ox and Fe exhibit a better correlation when focusing on the bottom third of the cloud (R^2_{adj}
1113 = 0.29 and $R^2_{adj} = 0.20$ for Ox and Fe, respectively). When focusing on the top third of the cloud,
1114 the correlation decreased for Ox ($R^2_{adj} = 0.08$) and remained unchanged for Fe ($R^2_{adj} = 0.03$). One
1115 possible hypothesis to explain why Ox and Fe are better predictors of N_d at cloud base is that
1116 smokes affects cloud microphysics (N_d and effective radius) more at cloud base than at cloud top,
1117 regardless of whether the smoke was above or below the cloud (Diamond et al., 2018; Mardi et
1118 al., 2019).

1119 NSS-SO₄²⁻ and Na exhibit a better correlation with N_d when focusing on the top third of
1120 the cloud ($R^2_{adj} = 0.33$ and $R^2_{adj} = 0.33$ for NSS-SO₄²⁻ and Na, respectively). The correlation
1121 decreases when focusing on the bottom third of the cloud ($R^2_{adj} = 0.17$ and $R^2_{adj} = 0.10$ for NSS-
1122 SO₄²⁻ and Na, respectively). Tot-SO₄²⁻ also follows this pattern ($R^2_{adj} = 0.56$ and $R^2_{adj} = 0.22$ for
1123 top and bottom, respectively).

1124 It is not entirely clear why NSS-SO₄²⁻ and Na would be better correlated with N_d in the top
1125 third of clouds. MacDonald et al. (2018) noted that the concentration of chemical species varies as
1126 a function of in-cloud height and is not the same for all species; the concentration of Na is greatest
1127 at cloud base whereas that of NSS-SO₄²⁻ and Ox are greatest mid-cloud. It would be expected that
1128 the vertical profile of concentration is related to the ability to predict N_d (i.e., that a larger
1129 concentration of a species leads to a better correlation with N_d), but that expectation is not observed
1130 in these results. It is also interesting to point out that there is not much difference in R^2_{adj} when
1131 considering all cloud thirds versus only the middle third; this makes sense, as almost half of the
1132 cloud water samples (46%) were collected in the middle third of the cloud.

1133 The dependence of the correlation between chemical composition and N_d on in-cloud
1134 height is of relevance to remote sensing, which relies on satellite measurement of cloud top
1135 properties such as cloud top temperature to then calculate a constant N_d throughout the cloud depth
1136 (e.g., Grosvenor et al., 2018).

1137

1138 4. Conclusions

1139 This study used a four-year data set of airborne measurements collected in warm marine
1140 stratocumulus clouds off the California coast and analyzed the extent to which the chemical
1141 composition of cloud water can be used to predict N_d . A total of 7980 species were filtered to nine
1142 to examine the prediction of N_d using a single-species model, and then using a multi-species model.
1143 The 799 species were subsequently filtered to four to examine how the four single-species
1144 models were affected by environmental factors, namely, turbulence, smoke influence, and vertical
1145 location within a cloud. The most important findings of this paper are:

1146

- 1147 1. The species that best predicted N_d is Tot-SO₄²⁻ with $R^2_{adj} = 0.40$, followed by NH₄⁺ ($R^2_{adj} =$
1148 0.34), NSS-SO₄²⁻ ($R^2_{adj} = 0.29$), MSA ($R^2_{adj} = 0.26$), and NO₃⁻ ($R^2_{adj} = 0.24$).
- 1149 2. The prediction of N_d can be improved by using a multi-species model. However, increasing
1150 the number of species caused the R^2_{adj} to asymptotically approach ~ 0.6. Furthermore, the
1151 regressions with six or more species became statistically insignificant.
- 1152 3. Analyzing the three best correlations for each of the n-species models (where n = 1—5) shows
1153 that the factors that constitute a good regression are: a form of SO₄²⁻ (total or non-sea salt), an
1154 ocean emissions tracer, and an organic tracer.
- 1155 4. Greater turbulence (approximated as the standard deviation of vertical wind speed) improves
1156 the ability of ocean-derived species to predict N_d , as observed when comparing regressions

1157 using turbulent data points versus all data points for Tot-SO₄²⁻ ($\Delta R^2_{adj} = 0.15$) and Na (ΔR^2_{adj}
1158 $= 0.07$), but not for NSS-SO₄²⁻ ($\Delta R^2_{adj} = -0.01$) or Ox ($\Delta R^2_{adj} = -0.06$).
1159 5. The influence of smoke significantly affects those species that best predict N_d . Ox (a species
1160 known to be produced during biomass burning) was best correlated with N_d ($R^2_{adj} = 0.42$) under
1161 smoke-influenced conditions.
1162 6. Vertical location within the cloud affects the ability to predict N_d . The species that are best
1163 correlated with N_d at cloud top are Tot-SO₄²⁻ ($R^2_{adj} = 0.56$) and NSS-SO₄²⁻ ($R^2_{adj} = 0.33$); those
1164 best correlated with N_d at cloud base are fire tracers such as Ox ($R^2_{adj} = 0.29$) and Fe ($R^2_{adj} =$
1165 0.20), as it has been reported that the base of a cloud is more sensitive to the influence of
1166 smoke.

1167 **Data Availability**
1168 All data used in this work can be found on the Figshare database (Sorooshian et al., ~~2018;~~
1169 ~~https~~2017; [https://figshare.com/articles/A_Multi-Year_Data_Set_on_Aerosol-Cloud-
1171 Precipitation-Meteorology_Interactions_for_Marine_Stratocumulus_Clouds/5099983](https://figshare.com/articles/A_Multi-Year_Data_Set_on_Aerosol-Cloud-
1170 Precipitation-Meteorology_Interactions_for_Marine_Stratocumulus_Clouds/5099983)).
1172 **Author Contributions**
1173 All coauthors contributed to some aspect of the data collection. ABM and AS conducted
1174 the data analysis and interpretation. ABM and AS prepared the manuscript with contributions from
1175 all coauthors.
1176 **Competing Interests**
1177 The authors declare that they have no conflict of interest.
1178
1179 **Acknowledgements**
1180 Alexander B. MacDonald acknowledges support from the Mexican National Council for
1181 Science and Technology (CONACYT). We acknowledge Agilent Technologies for their support
1182 and Shane Snyder's laboratories for ICP-QQQ data.
1183
1184 **Financial Support**
1185 These field campaigns were funded by Office of Naval Research grants N00014-10-1-
1186 0811, N00014-11-1-0783, N00014-10-1-0200, N00014-04-1-0118, and N00014-16-1-2567. This
1187 work was also partially supported by NASA grant 80NSSC19K0442 in support of the ACTIVATE
1188 Earth Venture Suborbital-3 (EVS-3) investigation, which is funded by NASA's Earth Science
1189 Division and managed through the Earth System Science Pathfinder Program Office.
1190
1191
1192

- 1193 **References**
- 1194 Abdul-Razzak, H. and Ghan, S. J.: A parameterization of aerosol activation 2. Multiple aerosol
- 1195 types, *J. Geophys. Res.*, 105(D5), 6837–6844, <https://doi.org/10.1029/1999JD901161>,
- 1196 2000.
- 1197 [Ackerman, A. S., Kirkpatrick, M. P., Stevens, D. E., and Toon, O. B.: The impact of humidity](https://doi.org/10.1038/nature03174)
- 1198 [above stratiform clouds on indirect aerosol climate forcing, *Nature*, 432\(7020\), 1014–](https://doi.org/10.1038/nature03174)
- 1199 [1017, *https://doi.org/10.1038/nature03174*, 2004.](https://doi.org/10.1038/nature03174)
- 1200 Adams, P. J. and Seinfeld, J. H.: Disproportionate impact of particulate emissions on global
- 1201 cloud condensation nuclei concentrations, *Geophys. Res. Lett.*, 30(5), 1239,
- 1202 <https://doi.org/10.1029/2002gl016303>, 2003.
- 1203 Albrecht, B. A.: Aerosols, Cloud Microphysics, and Fractional Cloudiness, *Science*, 245(4923),
- 1204 1227–1230, <https://doi.org/10.1126/science.245.4923.1227>, 1989.
- 1205 Andreae, M. O. and Rosenfeld, D.: Aerosol-cloud-precipitation interactions. Part 1. The nature
- 1206 and sources of cloud-active aerosols, *Earth-Science Rev.*, 89(1–2), 13–41,
- 1207 <https://doi.org/10.1016/j.earscirev.2008.03.001>, 2008.
- 1208 ApSimon, H. M., Kruse, M. and Bell, J. N. B.: Ammonia emissions and their role in acid
- 1209 deposition, *Atmos. Environ.*, 21(9), 1939–1946, [https://doi.org/10.1016/0004-](https://doi.org/10.1016/0004-6981(87)90154-5)
- 1210 [6981\(87\)90154-5](https://doi.org/10.1016/0004-6981(87)90154-5), 1987.
- 1211 Bauer, S. E., Tsigaridis, K. and Miller, R.: Significant atmospheric aerosol pollution caused by
- 1212 world food cultivation, *Geophys. Res. Lett.*, 43(10), 5394–5400,
- 1213 <https://doi.org/10.1002/2016GL068354>, 2016.
- 1214 Baumgardner, D., Jonsson, H., Dawson, W., O’Connor, D. and Newton, R.: The cloud, aerosol
- 1215 and precipitation spectrometer: A new instrument for cloud investigations, *Atmos. Res.*,
- 1216 59–60, 251–264, [https://doi.org/10.1016/S0169-8095\(01\)00119-3](https://doi.org/10.1016/S0169-8095(01)00119-3), 2001.
- 1217 Behrenfeld, M. J., Moore, R. H., Hostetler, C. A., Graff, J., Gaube, P., Russell, L. M., Chen, G.,
- 1218 Doney, S. C., Giovannoni, S., Liu, H., Proctor, C., Bolaños, L. M., Baetge, N., Davie-
- 1219 Martin, C., Westberry, T. K., Bates, T. S., Bell, T. G., Bidle, K. D., Boss, E. S., Brooks, S.
- 1220 D., Cairns, B., Carlson, C., Halsey, K., Harvey, E. L., Hu, C., Karp-Boss, L., Kleb, M.,
- 1221 Menden-Deuer, S., Morison, F., Quinn, P. K., Scarino, A. J., Anderson, B., Chowdhary,
- 1222 J., Crosbie, E., Ferrare, R., Hair, J. W., Hu, Y., Janz, S., Redemann, J., Saltzman, E.,
- 1223 Shook, M., Siegel, D. A., Wisthaler, A., Martin, M. Y. and Ziemba, L.: The North Atlantic
- 1224 Aerosol and Marine Ecosystem Study (NAAMES): Science motive and mission overview,
- 1225 *Front. Mar. Sci.*, 6, 1–25, <https://doi.org/10.3389/fmars.2019.00122>, 2019.
- 1226 [Bellouin, N., Quaas, J., Gryspeerdt, E., Kinne, S., Stier, P., Watson-Parris, D., Boucher, O.,](https://doi.org/10.1029/2019rg000660)
- 1227 [Carslaw, K. S., Christensen, M., Daniaou, A.-L., Dufresne, J.-L., Feingold, G., Fiedler, S.,](https://doi.org/10.1029/2019rg000660)
- 1228 [Forster, P., Gettelman, A., Haywood, J. M., Lohmann, U., Malavelle, F., Mauritsen, T.,](https://doi.org/10.1029/2019rg000660)
- 1229 [McCoy, D. T., Myhre, G., Mülmenstädt, J., Neubauer, D., Possner, A., Rugenstein, M.,](https://doi.org/10.1029/2019rg000660)
- 1230 [Sato, Y., Schulz, M., Schwartz, S. E., Sourdeval, O., Storelvmo, T., Toll, V., Winker, D.,](https://doi.org/10.1029/2019rg000660)
- 1231 [and Stevens, B.: Bounding Global Aerosol Radiative Forcing of Climate Change, *Rev.*](https://doi.org/10.1029/2019rg000660)
- 1232 [*Geophys.*, 58, e2019RG000660, *https://doi.org/10.1029/2019rg000660*, 2020.](https://doi.org/10.1029/2019rg000660)
- 1233 Borys, R. D., Lowenthal, D. H., Wetzell, M. A., Herrera, F., Gonzalez, A. and Harris, J.:
- 1234 Chemical and microphysical properties of marine stratiform cloud in the North Atlantic, *J.*
- 1235 *Geophys. Res. Atmos.*, 103(D17), 22073–22085, <https://doi.org/10.1029/98JD02087>,
- 1236 1998.
- 1237 Boucher, O. and Lohmann, U.: The sulfate-CCN-cloud albedo effect, *Tellus B Chem. Phys.*
- 1238 *Meteorol.*, 47(3), 281–300, <https://doi.org/10.3402/tellusb.v47i3.16048>, 1995.

1239 Bouwman, A. F., Lee, D. S., Asman, W. A. H., Dentener, F. J., Van Der Hoek, K. W. and
1240 Olivier, J. G. J.: A global high-resolution emission inventory for ammonia, *Global*
1241 *Biogeochem. Cycles*, 11(4), 561–587, <https://doi.org/10.1029/97GB02266>, 1997.

1242 Charlson, R. J., Lovelock, J. E., Andreae, M. O. and Warren, S. G.: Oceanic phytoplankton,
1243 atmospheric sulphur, cloud albedo and climate, *Nature*, 326(6114), 655–661,
1244 <https://doi.org/10.1038/326655a0>, 1987.

1245 Charlson, R. J., Schwartz, S. E., Hales, J. M., Cess, R. D., Coakley, J. J., Hansen, J. E. and
1246 Hofmann, D. J.: Climate forcing by anthropogenic aerosols, *Science*, 117(5043), 423–430,
1247 <https://doi.org/10.1126/science.255.5043.423>, 1992.

1248 Chen, Y. and Penner, J. E.: Uncertainty analysis for estimates of the first indirect aerosol effect,
1249 *Atmos. Chem. Phys.*, 5(11), 2935–2948, <https://doi.org/10.5194/acp-5-2935-2005>, 2005.

1250 Chen, Y.-C., Christensen, M. W., Xue, L., Sorooshian, A., Stephens, G. L., Rasmussen, R. M.
1251 and Seinfeld, J. H.: Occurrence of lower cloud albedo in ship tracks, *Atmos. Chem. Phys.*,
1252 12(17), 8223–8235, <https://doi.org/10.5194/acp-12-8223-2012>, 2012.

1253 Chuang, C. C., Penner, J. E. and Edwards, L. L.: Nucleation Scavenging of Smoke Particles and
1254 Simulated Drop Size Distributions over Large Biomass Fires, *J. Atmos. Sci.*, 49(14),
1255 1264–1276, [https://doi.org/10.1175/1520-0469\(1992\)049<1264:NSOSPA>2.0.CO;2](https://doi.org/10.1175/1520-0469(1992)049<1264:NSOSPA>2.0.CO;2),
1256 1992.

1257 Chuang, C. C. and Penner, J. E.: Effects of anthropogenic sulfate on cloud drop nucleation and
1258 optical properties, *Tellus B Chem. Phys. Meteorol.*, 47(5), 566–577,
1259 <https://doi.org/10.1034/j.1600-0889.47.issue5.4.x>, 1995.

1260 Coggon, M. M., Sorooshian, A., Wang, Z., Metcalf, A. R., Frossard, A. A., Lin, J. J., Craven, J.
1261 S., Nenes, A., Jonsson, H. H., Russell, L. M., Flagan, R. C. and Seinfeld, J. H.: Ship
1262 impacts on the marine atmosphere: Insights into the contribution of shipping emissions to
1263 the properties of marine aerosol and clouds, *Atmos. Chem. Phys.*, 12(18), 8439–8458,
1264 <https://doi.org/10.5194/acp-12-8439-2012>, 2012.

1265 Coggon, M. M., Sorooshian, A., Wang, Z., Craven, J. S., Metcalf, A. R., Lin, J. J., Nenes, A.,
1266 Jonsson, H. H., Flagan, R. C. and Seinfeld, J. H.: Observations of continental biogenic
1267 impacts on marine aerosol and clouds off the coast of California, *J. Geophys. Res. Atmos.*,
1268 119(11), 6724–6748, <https://doi.org/10.1002/2013JD021228>, 2014.

1269 Crosbie, E., Wang, Z., Sorooshian, A., Chuang, P. Y., Craven, J. S., Coggon, M. M., Brunke, M.,
1270 Zeng, X., Jonsson, H., Woods, R. K., Flagan, R. C. and Seinfeld, J. H.: Stratocumulus
1271 Cloud Clearings and Notable Thermodynamic and Aerosol Contrasts across the Clear–
1272 Cloudy Interface, *J. Atmos. Sci.*, 73(3), 1083–1099, <https://doi.org/10.1175/JAS-D-15-0137.1>, 2016.

1274 Dadashazar, H., Wang, Z., Crosbie, E., Brunke, M., Zeng, X., Jonsson, H., Woods, R. K.,
1275 Flagan, R. C., Seinfeld, J. H. and Sorooshian, A.: Relationships between giant sea salt
1276 particles and clouds inferred from aircraft physicochemical data, *J. Geophys. Res.*, 122(6),
1277 3421–3434, <https://doi.org/10.1002/2016JD026019>, 2017.

1278 Dadashazar, H., Ma, L. and Sorooshian, A.: Sources of pollution and interrelationships between
1279 aerosol and precipitation chemistry at a central California site, *Sci. Total Environ.*, 651,
1280 1776–1787, <https://doi.org/10.1016/j.scitotenv.2018.10.086>, 2019.

1281 Diamond, M. S., Dobracki, A., Freitag, S., Griswold, J. D. S., Heikkila, A., Howell, S. G.,
1282 Kacarab, M. E., Podolske, J. R., Saide, P. E. and Wood, R.: Time-dependent entrainment
1283 of smoke presents an observational challenge for assessing aerosol-cloud interactions over

1284 the southeast Atlantic Ocean, *Atmos. Chem. Phys.*, 18(19), 14623–14636,
1285 <https://doi.org/10.5194/acp-18-14623-2018>, 2018.

1286 Facchini, M. C., Mircea, M., Fuzzi, S. and Charlson, R. J.: Cloud albedo enhancement by
1287 surface-active organic solutes in growing droplets, *Nature*, 401(6750), 257–259,
1288 <https://doi.org/10.1038/45758>, 1999.

1289 Feingold, G., Frisch, A. S., Stevens, B. and Cotton, W. R.: On the relationship among cloud
1290 turbulence, droplet formation and drizzle as viewed by Doppler radar, microwave
1291 radiometer and lidar, *J. Geophys. Res. Atmos.*, 104(D18), 22195–22203,
1292 <https://doi.org/10.1029/1999JD900482>, 1999.

1293 Feingold, G., Cotton, W. R., Kreidenweis, S. M. and Davis, J. T.: The Impact of Giant Cloud
1294 Condensation Nuclei on Drizzle Formation in Stratocumulus: Implications for Cloud
1295 Radiative Properties, *J. Atmos. Sci.*, 56, 4100–4117, [http://doi.org/10.1175/1520-](http://doi.org/10.1175/1520-0469(1999)056<4100:TIOGCC>2.0.CO;2)
1296 [0469\(1999\)056<4100:TIOGCC>2.0.CO;2](http://doi.org/10.1175/1520-0469(1999)056<4100:TIOGCC>2.0.CO;2), 1999.

1297 Fountoukis, C. and Nenes, A.: Continued development of a cloud droplet formation
1298 parameterization for global climate models, *J. Geophys. Res. Atmos.*, 110(D11), D11212,
1299 <https://doi.org/10.1029/2004JD005591>, 2005.

1300 Freund, R. J., Wilson, W. J. and Mohr, D. L.: *Statistical Methods*, 3rd ed., Academic Press,
1301 Burlington, MA., 2010.

1302 Gelaro, R., McCarty, W., Suárez, M. J., Todling, R., Molod, A., Takacs, L., Randles, C. A.,
1303 Darmenov, A., Bosilovich, M. G., Reichle, R., Wargan, K., Coy, L., Cullather, R., Draper,
1304 C., Akella, S., Buchard, V., Conaty, A., da Silva, A. M., Gu, W., Kim, G. K., Koster, R.,
1305 Lucchesi, R., Merkova, D., Nielsen, J. E., Partyka, G., Pawson, S., Putman, W.,
1306 Rienecker, M., Schubert, S. D., Sienkiewicz, M. and Zhao, B.: The modern-era
1307 retrospective analysis for research and applications, version 2 (MERRA-2), *J. Clim.*,
1308 30(14), 5419–5454, <https://doi.org/10.1175/JCLI-D-16-0758.1>, 2017.

1309 Gerber, H., Arends, B. G. and Ackerman, A. S.: New microphysics sensor for aircraft use,
1310 *Atmos. Res.*, 31(4), 235–252, [https://doi.org/10.1016/0169-8095\(94\)90001-9](https://doi.org/10.1016/0169-8095(94)90001-9), 1994.

1311 Gerber, H., Frick, G. and Rodi, A. R.: Ground-based FSSP and PVM measurements of liquid
1312 water content, *J. Atmos. Ocean. Technol.*, 16(8), 1143–1149,
1313 [https://doi.org/10.1175/1520-0426\(1999\)016<1143:GBFAPM>2.0.CO;2](https://doi.org/10.1175/1520-0426(1999)016<1143:GBFAPM>2.0.CO;2), 1999.

1314 Ghan, S. J., Leung, L. R. and Easter, R. C.: Prediction of cloud droplet number in a general
1315 circulation model, *J. Geophys. Res.*, 102(D18), 21777–21794,
1316 <https://doi.org/10.1029/97JD01810>, 1997.

1317 Ghan, S. J., Abdul-Razzak, H., Nenes, A., Ming, Y., Liu, X., Ovchinnikov, M., Shipway, B.,
1318 Meskhidze, N., Xu, J. and Shi, X.: Droplet nucleation: Physically-based parameterizations
1319 and comparative evaluation, *J. Adv. Model. Earth Syst.*, 3(4), 1–34,
1320 <https://doi.org/10.1029/2011ms000074>, 2011.

1321 Gong, S. L.: A parameterization of sea-salt aerosol source function for sub- and super-micron
1322 particles, *Global Biogeochem. Cycles*, 17(4), 1097, <https://doi.org/2003gb002079>, 2003.

1323 Grosvenor, D. P., Sourdeval, O., Zuidema, P., Ackerman, A., Alexandrov, M. D., Bennartz, R.,
1324 Boers, R., Cairns, B., Chiu, J. C., Christensen, M., Deneke, H., Diamond, M., Feingold,
1325 G., Fridlind, A., Hünerbein, A., Knist, C., Kollias, P., Marshak, A., McCoy, D., Merk, D.,
1326 Painemal, D., Rausch, J., Rosenfeld, D., Russchenberg, H., Seifert, P., Sinclair, K., Stier,
1327 P., van Diedenhoven, B., Wendisch, M., Werner, F., Wood, R., Zhang, Z. and Quaas, J.:
1328 Remote Sensing of Droplet Number Concentration in Warm Clouds: A Review of the

1329 Current State of Knowledge and Perspectives, *Rev. Geophys.*, 56(2), 409–453,
 1330 <https://doi.org/10.1029/2017RG000593>, 2018.
 1331 Hegg, D. A.: Impact of gas-phase HNO₃ and NH₃ on microphysical processes in atmospheric
 1332 clouds, *Geophys. Res. Lett.*, 27(15), 2201–2204, <https://doi.org/10.1029/1999GL011252>,
 1333 2000.
 1334 Hegg, D. A. and Hobbs, P. V.: Cloud Water Chemistry and the production of sulfates in clouds,
 1335 *Atmos. Environ.*, 15(9), 1597–1604, [https://doi.org/10.1016/0004-6981\(81\)90144-X](https://doi.org/10.1016/0004-6981(81)90144-X),
 1336 1981.
 1337 Hegg, D. A. and Hobbs, P. V.: Sulfate and nitrate chemistry in cumuliform clouds, *Atmos.*
 1338 *Environ.*, 20(5), 901–909, [https://doi.org/10.1016/0004-6981\(86\)90274-X](https://doi.org/10.1016/0004-6981(86)90274-X), 1986.
 1339 Hegg, D. A., Ferek, R. J. and Hobbs, P. V.: Light scattering and cloud condensation nucleus
 1340 activity of sulfate aerosol measured over the northeast Atlantic Ocean, *J. Geophys. Res.*
 1341 *Atmos.*, 98(D8), 14887–14894, <https://doi.org/10.1029/93JD01615>, 1993.
 1342 Hersey, S. P., Sorooshian, A., Murphy, S. M., Flagan, R. C. and Seinfeld, J. H.: Aerosol
 1343 hygroscopicity in the marine atmosphere: a closure study using high-resolution, size-
 1344 resolved AMS and multiple-RH DASH-SP data, *Atmos. Chem. Phys.*, 9(7), 16789–16817,
 1345 <https://doi.org/10.5194/acpd-8-16789-2008>, 2009.
 1346 Hudson, P. K., Murphy, D. M., Cziczo, D. J., Thomson, D. S., de Gouw, J. A., Warneke, C.,
 1347 Holloway, J., Jost, H. J. and Hübler, G.: Biomass-burning particle measurements:
 1348 Characteristics composition and chemical processing, *J. Geophys. Res. Atmos.*, 109,
 1349 D23S27, <https://doi.org/10.1029/2003JD004398>, 2004.
 1350 Intergovernmental Panel on Climate Change: Climate Change 2007: The Physical Science Basis.
 1351 Contribution of Working Group I to the Fourth Assessment Report of the
 1352 Intergovernmental Panel on Climate Change, Cambridge University Press, Cambridge,
 1353 United Kingdom and New York, NY, USA., 2007.
 1354 Intergovernmental Panel on Climate Change: Climate Change 2013: The Physical Science Basis.
 1355 Contribution of Working Group I to the Fifth Assessment Report of the Intergovernmental
 1356 Panel on Climate Change, Cambridge University Press, Cambridge, United Kingdom and
 1357 New York, NY, USA., 2013.
 1358 [Jung, E., Albrecht, B. A., Jonsson, H. H., Chen, Y.-C., Seinfeld, J. H., Sorooshian, A., Metcalf,](https://doi.org/10.5194/acp-15-5645-2015)
 1359 [A. R., Song, S., Fang, M. and Russell, L. M.: Precipitation effects of giant cloud](https://doi.org/10.5194/acp-15-5645-2015)
 1360 [condensation nuclei artificially introduced into stratocumulus clouds, *Atmos. Chem.*](https://doi.org/10.5194/acp-15-5645-2015)
 1361 [*Phys.*, 15, 5645–5658, <http://doi.org/10.5194/acp-15-5645-2015>, 2015.](https://doi.org/10.5194/acp-15-5645-2015)
 1362 Jickells, T. D., An, Z. S., Andersen, K. K., Baker, A. R., Bergametti, G., Brooks, N., Cao, J. J.,
 1363 Boyd, P. W., Duce, R. A., Hunter, K. A., Kawahata, H., Kubilay, N. and Liss, P. S.:
 1364 Global Iron Connections Between Desert Dust, Ocean Biogeochemistry, and Climate,
 1365 *Science*, 308(5718), 67–71, <https://doi.org/10.1126/science.1105959>, 2005.
 1366 Kahane, L. H.: Regression Basics, 2nd ed., Sage Publications, Thousand Oaks, CA., 2008.
 1367 Koch, D. and Del Genio, A. D.: Black carbon semi-direct effects on cloud cover: Review and
 1368 synthesis, *Atmos. Chem. Phys.*, 10(16), 7685–7696, [https://doi.org/10.5194/acp-10-7685-](https://doi.org/10.5194/acp-10-7685-2010)
 1369 2010, 2010.
 1370 Kulmala, M., Laaksonen, A., Korhonen, P., Vesala, T., Ahonen, T. and Barrett, J. C.: The effect
 1371 of atmospheric nitric acid vapor on cloud condensation nucleus activation, *J. Geophys.*
 1372 *Res.*, 98(D12), 22949–22958, <https://doi.org/10.1029/93JD02070>, 1993.
 1373 Lance, S., Nenes, A., Mazzoleni, C., Dubey, M. K., Gates, H., Varutbangkul, V., Rissman, T. A.,
 1374 Murphy, S. M., Sorooshian, A., Flagan, R. C., Seinfeld, J. H., Feingold, G. and Jonsson,

1375 H. H.: Cloud condensation nuclei activity, closure, and droplet growth kinetics of Houston
1376 aerosol during the Gulf of Mexico Atmospheric Composition and Climate Study
1377 (GoMACCS), *J. Geophys. Res.*, 114, D00F15, <https://doi.org/10.1029/2008jd011699>,
1378 2009.

1379 Leaitch, W. R., Strapp, J. W., Wiebe, H. A., Anlauf, K. G. and Isaac, G. A.: Chemical and
1380 microphysical studies of nonprecipitating summer cloud in Ontario, Canada, *J. Geophys.*
1381 *Res. Atmos.*, 91(D11), 11821–11831, <https://doi.org/10.1029/JD091iD11p11821>, 1986.

1382 Leaitch, W. R., Isaac, G. A., Strapp, J. W., Banic, C. M. and Wiebe, H. A.: The relationship
1383 between cloud droplet number concentrations and anthropogenic pollution: observations
1384 and climatic implications, *J. Geophys. Res. Atmos.*, 97(D2), 2463–2474,
1385 <https://doi.org/10.1029/91JD02739>, 1992.

1386 Leaitch, W. R., Banic, C. M., Isaac, G. A., Couture, M. D., Liu, P. S. K., Gultepe, I., Li, S. M.,
1387 Kleinman, L., Daum, P. H. and MacPherson, J. I.: Physical and chemical observations in
1388 marine stratus during the 1993 North Atlantic Regional Experiment: Factors controlling
1389 cloud droplet number concentrations, *J. Geophys. Res. Atmos.*, 101(D22), 29123–29135,
1390 <https://doi.org/10.1029/96JD01228>, 1996.

1391 Lowenthal, D. H. and Borys, R. D.: Sources of microphysical variation in marine stratiform
1392 clouds in the North Atlantic, *Geophys. Res. Lett.*, 27(10), 1491–1494,
1393 <https://doi.org/10.1029/1999GL010992>, 2000.

1394 Lowenthal, D. H., Borys, R. D., Choulaton, T. W., Bower, K. N., Flynn, M. J. and Gallagher,
1395 M. W.: Parameterization of the cloud droplet–sulfate relationship, *Atmos. Environ.*, 38(2),
1396 287–292, <https://doi.org/10.1016/j.atmosenv.2003.09.046>, 2004.

1397 Lu, M. L., Sorooshian, A., Jonsson, H. H., Feingold, G., Flagan, R. C. and Seinfeld, J. H.:
1398 Marine stratocumulus aerosol-cloud relationships in the MASE-II experiment:
1399 Precipitation susceptibility in eastern Pacific marine stratocumulus, *J. Geophys. Res.*
1400 *Atmos.*, 114(24), 1–11, <https://doi.org/10.1029/2009JD012774>, 2009.

1401 [Ma, L., Dadashazar, H., Braun, R. A., MacDonald, A. B., Aghdam, M. A., Maudlin, L. C. and](https://doi.org/10.1016/j.atmosenv.2019.02.045)
1402 [Sorooshian, A.: Size-resolved characteristics of water-soluble particulate elements in a](https://doi.org/10.1016/j.atmosenv.2019.02.045)
1403 [coastal area: Source identification, influence of wildfires, and diurnal variability, *Atmos.*](https://doi.org/10.1016/j.atmosenv.2019.02.045)
1404 [*Environ.*, 206, 72–84, <https://doi.org/10.1016/j.atmosenv.2019.02.045>, 2019.](https://doi.org/10.1016/j.atmosenv.2019.02.045)

1405 MacDonald, A. B., Dadashazar, H., Chuang, P. Y., Crosbie, E., Wang, H., Wang, Z., Jonsson, H.
1406 H., Flagan, R. C., Seinfeld, J. H. and Sorooshian, A.: Characteristic Vertical Profiles of
1407 Cloud Water Composition in Marine Stratocumulus Clouds and Relationships with
1408 Precipitation, *J. Geophys. Res. Atmos.*, 123(7), 3704–3723,
1409 <https://doi.org/10.1002/2017JD027900>, 2018.

1410 Mardi, A. H., Dadashazar, H., MacDonald, A. B., Braun, R. A., Crosbie, E., Xian, P., Thorsen,
1411 T. J., Coggon, M. M., Fenn, M. A., Ferrare, R. A., Hair, J. W., Woods, R. K., Jonsson, H.
1412 H., Flagan, R. C., Seinfeld, J. H. and Sorooshian, A.: Biomass Burning Plumes in the
1413 Vicinity of the California Coast: Airborne Characterization of Physicochemical Properties,
1414 Heating Rates, and Spatiotemporal Features, *J. Geophys. Res. Atmos.*, 123(23), 13560–
1415 13582, <https://doi.org/10.1029/2018JD029134>, 2018.

1416 Mardi, A. H., Dadashazar, H., MacDonald, A. B., Crosbie, E., Coggon, M. M., Aghdam, M. A.,
1417 Woods, R. K., Jonsson, H. H., Flagan, R. C., Seinfeld, J. H. and Sorooshian, A.: Effects of
1418 Biomass Burning on Stratocumulus Droplet Characteristics, Drizzle Rate, and
1419 Composition, *J. Geophys. Res. Atmos.*, 124(22), 12301–12318,
1420 <https://doi.org/10.1029/2019JD031159>, 2019.

1421 Matsumoto, K., Tanaka, H., Nagao, I. and Ishizaka, Y.: Contribution of particulate sulfate and
 1422 organic carbon to cloud condensation nuclei in the marine atmosphere, *Geophys. Res.
 1423 Lett.*, 24(6), 655–658, <https://doi.org/10.1029/97GL00541>, 1997.
 1424 Maudlin, L. C., Wang, Z., Jonsson, H. H. and Sorooshian, A.: Impact of wildfires on size-
 1425 resolved aerosol composition at a coastal California site, *Atmos. Environ.*, 119, 59–68,
 1426 <https://doi.org/10.1016/j.atmosenv.2015.08.039>, 2015.
 1427 McCoy, D. T., Bender, F. A.-M., Mohrmann, J. K. C., Hartmann, D. L., Wood, R. and
 1428 Grosvenor, D. P.: The global aerosol-cloud first indirect effect estimated using MODIS,
 1429 MERRA, and AeroCom, *J. Geophys. Res. Atmos.*, 122(3), 1779–1796,
 1430 <https://doi.org/10.1002/2016JD026141>, 2017.
 1431 McCoy, D. T., Bender, F. A.-M., Grosvenor, D. P., Mohrmann, J. K., Hartmann, D. L., Wood, R.
 1432 and Field, P. R.: Predicting decadal trends in cloud droplet number concentration using
 1433 reanalysis and satellite data, *Atmos. Chem. Phys.*, 18(3), 2035–2047,
 1434 <https://doi.org/10.5194/acp-18-2035-2018>, 2018.
 1435 Medina, J., Nenes, A., Sotiropoulou, R. E. P., Cottrell, L. D., Ziemba, L. D., Beckman, P. J. and
 1436 Griffin, R. J.: Cloud condensation nuclei closure during the International Consortium for
 1437 Atmospheric Research on Transport and Transformation 2004 campaign: Effects of size-
 1438 resolved composition, *J. Geophys. Res. Atmos.*, 112(D10), D10S31,
 1439 <https://doi.org/10.1029/2006JD007588>, 2007.
 1440 Menon, S. and Saxena, V. K.: Role of sulfates in regional cloud–climate interactions, *Atmos.
 1441 Res.*, 47–48, 299–315, [https://doi.org/https://doi.org/10.1016/S0169-8095\(98\)00057-X](https://doi.org/https://doi.org/10.1016/S0169-8095(98)00057-X),
 1442 1998.
 1443 Menon, S., Genio, A. D. Del, Koch, D. and Tselioudis, G.: GCM Simulations of the Aerosol
 1444 Indirect Effect: Sensitivity to Cloud Parameterization and Aerosol Burden, *J. Atmos. Sci.*,
 1445 59(3), 692–713, [https://doi.org/10.1175/1520-0469\(2002\)059<0692:gsotai>2.0.co;2](https://doi.org/10.1175/1520-0469(2002)059<0692:gsotai>2.0.co;2),
 1446 2002.
 1447 Nenes, A., Charlson, R. J., Facchini, M. C., Kulmala, M., Laaksonen, A. and Seinfeld, J. H.: Can
 1448 chemical effects on cloud droplet number rival the first indirect effect?, *Geophys. Res.
 1449 Lett.*, 29(17), 1848, <https://doi.org/10.1029/2002gl015295>, 2002.
 1450 Nenes, A. and Seinfeld, J. H.: Parameterization of cloud droplet formation in global climate
 1451 models, *J. Geophys. Res. Atmos.*, 108(D14), 1–14, <https://doi.org/10.1029/2002jd002911>,
 1452 2003.
 1453 Novakov, T. and Penner, J. E.: Large contribution of organic aerosols to cloud-condensation-
 1454 nuclei concentrations, *Nature*, 365(6449), 823–826, <https://doi.org/10.1038/365823a0>,
 1455 1993.
 1456 Novakov, T., Rivera-Carpio, C., Penner, J. E. and Rogers, C. F.: The effect of anthropogenic
 1457 sulfate aerosols on marine cloud droplet concentrations, *Tellus B Chem. Phys. Meteorol.*,
 1458 46(2), 132–141, <https://doi.org/10.3402/tellusb.v46i2.15758>, 1994.
 1459 Partridge, D. G., Vrugt, J. A., Tunved, P., Ekman, A. M. L., Struthers, H. and Sorooshian, A.:
 1460 Inverse modelling of cloud-aerosol interactions - Part 2: Sensitivity tests on liquid phase
 1461 clouds using a Markov chain Monte Carlo based simulation approach, *Atmos. Chem.
 1462 Phys.*, 12(6), 2823–2847, <https://doi.org/10.5194/acp-12-2823-2012>, 2012.
 1463 Paulot, F., Jacob, D. J., Johnson, M. T., Bell, T. G., Baker, A. R., Keene, W. C., Lima, I. D.,
 1464 Doney, S. C. and Stock, C. A.: Global oceanic emission of ammonia: Constraints from
 1465 seawater and atmospheric observations, *Global Biogeochem. Cycles*, 29(8), 1165–1178,
 1466 <https://doi.org/10.1002/2015GB005106>, 2015.

1467 Prabhakar, G., Ervens, B., Wang, Z., Maudlin, L. C., Coggon, M. M., Jonsson, H. H., Seinfeld, J.
1468 H. and Sorooshian, A.: Sources of nitrate in stratocumulus cloud water: Airborne
1469 measurements during the 2011 E-PEACE and 2013 NiCE studies, *Atmos. Environ.*, 97,
1470 166–173, <https://doi.org/10.1016/j.atmosenv.2014.08.019>, 2014.

1471 Pringle, K. J., Carslaw, K. S., Spracklen, D. V., Mann, G. M. and Chipperfield, M. P.: The
1472 relationship between aerosol and cloud drop number concentrations in a global aerosol
1473 microphysics model, *Atmos. Chem. Phys.*, 9(12), 4131–4144, <https://doi.org/10.5194/acp-9-4131-2009>, 2009.

1475 Pueschel, R. F., Valin, C. C., Castillo, R. C., Kadlecsek, J. A. and Ganor, E.: Aerosols in polluted
1476 versus nonpolluted air masses: long-range transport and effects on clouds, *J. Appl.
1477 Meteorol. Clim.*, 25, 1908–1917, [https://doi.org/10.1175/1520-0450\(1986\)025<1908:AIPVNA>2.0.CO;2](https://doi.org/10.1175/1520-0450(1986)025<1908:AIPVNA>2.0.CO;2), 1986.

1479 [Pye, H. O. T., Nenes, A., Alexander, B., Ault, A. P., Barth, M. C., Clegg, S. L., Collett Jr., J. L.,
1480 Fahey, K. M., Hennigan, C. J., Herrmann, H., Kanakidou, M., Kelly, J. T., Ku, I.-T.,
1481 McNeill, V. F., Riemer, N., Schaefer, T., Shi, G., Tilgner, A., Walker, J. T., Wang, T.,
1482 Weber, R., Xing, J., Zaveri, R. A. and Zuend, A.: The acidity of atmospheric particles and
1483 clouds, *Atmos. Chem. Phys.*, 20\(8\), 4809–4888, <https://doi.org/10.5194/acp-20-4809-2020>, 2020.](#)

1484

1485 Quinn, P. K., Coffman, D. J., Johnson, J. E., Upchurch, L. M. and Bates, T. S.: Small fraction of
1486 marine cloud condensation nuclei made up of sea spray aerosol, *Nat. Geosci.*, 10(9), 674–
1487 679, <https://doi.org/10.1038/ngeo3003>, 2017.

1488 [Randles, C. A., da Silva, A. M., Buchard, V., Colarco, P. R., Darmenov, A., Govindaraju, R.,
1489 Smirnov, A., Holben, B., Ferrare, R., Hair, J., Shinozuka, Y. and Flynn, C. J.: The
1490 MERRA-2 aerosol reanalysis, 1980 onward. Part I: System description and data
1491 assimilation evaluation, *J. Clim.*, 30\(17\), 6823–6850, <https://doi.org/10.1175/JCLI-D-16-0609.1>, 2017.](#)

1492

1493 Reid, J. S., Hobbs, P. V., Ferek, R. J., Blake, D. R., Martins, J. V., Dunlap, M. R. and Liousse,
1494 C.: Physical, chemical, and optical properties of regional hazes dominated by smoke in
1495 Brazil, *J. Geophys. Res. Atmos.*, 103(D24), 32059–32080,
1496 <https://doi.org/10.1029/98JD00458>, 1998.

1497 Russell, L. M., Sorooshian, A., Seinfeld, J. H., Albrecht, B. A., Nenes, A., Ahlm, L., Chen, Y.-
1498 C., Coggon, M., Craven, J. S., Flagan, R. C., Frossard, A. A., Jonsson, H., Jung, E., Lin, J.
1499 J., Metcalf, A. R., Modini, R., Mülmenstädt, J., Roberts, G. C., Shingler, T., Song, S.,
1500 Wang, Z. and Wonaschütz, A.: Eastern pacific emitted aerosol cloud experiment, *Bull.
1501 Am. Meteorol. Soc.*, 94(5), 709–729, <https://doi.org/10.1175/BAMS-D-12-00015.1>, 2013.

1502 Saxena, V. K. and Menon, S.: Sulfate-induced cooling in the southeastern US: An observational
1503 assessment, *Geophys. Res. Lett.*, 26(16), 2489–2492,
1504 <https://doi.org/10.1029/1999GL900555>, 1999.

1505 Schlosser, J. S., Braun, R. A., Bradley, T., Dadashazar, H., MacDonald, A. B., Aldhaif, A. A.,
1506 Azadi Aghdam, M., Hossein Mardi, A., Xian, P. and Sorooshian, A.: Analysis of Aerosol
1507 Composition Data for Western United States Wildfires Between 2005-2015: Dust
1508 Emissions, Chloride Depletion, and Most Enhanced Aerosol Constituents, *J. Geophys.
1509 Res. Atmos.*, 122(16), 8951–8966, <https://doi.org/10.1002/2017JD026547>, 2017.

1510 [Schlosser, J. S., Dadashazar, H., Edwards, E.-L., Mardi, A. H., Prabhakar, G., Stahl, C., Jonsson,
1511 H. H. and Sorooshian, A.: Relationships between supermicrometer sea salt aerosol and](#)

1512 [marine boundary layer conditions: insights from repeated identical flight patterns, J.](#)
1513 [Geophys. Res. Atmos., accepted, <https://doi.org/10.1029/2019JD032346>, 2020.](#)

1514 Seinfeld, J. H. and Pandis, S. N.: Atmospheric Chemistry and Physics, 3rd ed., New York, NY.,
1515 2016.

1516 Silva, P. J., Liu, D. Y., Noble, C. A. and Prather, K. A.: Size and chemical characterization of
1517 individual particles resulting from biomass burning of local Southern California species,
1518 Environ. Sci. Technol., 33(18), 3068–3076, <https://doi.org/10.1021/es980544p>, 1999.

1519 Sorooshian, A., Lu, M. L., Brechtel, F. J., Jonsson, H., Feingold, G., Flagan, R. C. and Seinfeld,
1520 J. H.: On the source of organic acid aerosol layers above clouds, Environ. Sci. Technol.,
1521 41(13), 4647–4654, <https://doi.org/10.1021/es0630442>, 2007.

1522 Sorooshian, A., Padró, L. T., Nenes, A., Feingold, G., McComiskey, A., Hersey, S. P., Gates, H.,
1523 Jonsson, H. H., Miller, S. D., Stephens, G. L., Flagan, R. C. and Seinfeld, J. H.: On the
1524 link between ocean biota emissions, aerosol, and maritime clouds: Airborne, ground, and
1525 satellite measurements off the coast of California, Global Biogeochem. Cycles, 23(4), 1–
1526 15, <https://doi.org/10.1029/2009GB003464>, 2009.

1527 Sorooshian, A., MacDonald, A. B., Dadashazar, H., Bates, K. H., Coggon, M. M., Craven, J. S.,
1528 Crosbie, E., [Edwards, E.-L., Hersey, S. P., Hodas, N., Lin, J. J., Hossein Mardi, A., Marty,](#)
1529 [A. N., Maudlin, L. C., Metcalf, A. R., Murphy, S. M., Padro, L. T., Prabhakar, G.,](#)
1530 [Rissman, T. A., Schlosser, J., Shingler, T., Varutbangkul, V., Wang, Z., Woods, R. K.,](#)
1531 [Chuang, P. Y., Nenes, A., Jonsson, H. H., Flagan, R. C. and Seinfeld, J. H.: A multi-year](#)
1532 [data set on aerosol-cloud-precipitation-meteorology interactions for marine stratocumulus](#)
1533 [clouds, figshare, <https://doi.org/10.6084/m9.figshare.5099983.v10>, 2017.](#)

1534 [Sorooshian, A., MacDonald, A. B., Dadashazar, H., Bates, K. H., Coggon, M. M., Craven, J. S.,](#)
1535 [Crosbie, E., Hersey, S. P., Hodas, N., Lin, J. J., Negrón Marty, A., Maudlin, L. C.,](#)
1536 [Metcalf, A. R., Murphy, S. M., Padró, L. T., Prabhakar, G., Rissman, T. A., Shingler, T.,](#)
1537 [Varutbangkul, V., Wang, Z., Woods, R. K., Chuang, P. Y., Nenes, A., Jonsson, H. H.,](#)
1538 [Flagan, R. C. and Seinfeld, J. H.: A multi-year data set on aerosol-cloud-precipitation-](#)
1539 [meteorology interactions for marine stratocumulus clouds, Sci. Data, 5, 1–13,](#)
1540 <https://doi.org/10.1038/sdata.2018.26>, 2018.

1541 Sorooshian, A., Anderson, B., Bauer, S. E., Braun, R. A., Cairns, B., Crosbie, E., Dadashazar,
1542 H., Diskin, G., Ferrare, R., Flagan, R. C., Hair, J., Hostetler, C., Jonsson, H. H., Kleb, M.
1543 M., Liu, H., Macdonald, A. B., McComiskey, A., Moore, R., Painemal, D., Russell, L. M.,
1544 Seinfeld, J. H., Shook, M., Smith, W. L., Thornhill, K., Tselioudis, G., Wang, H., Zeng,
1545 X., Zhang, B., Ziemba, L. and Zuidema, P.: Aerosol–cloud–meteorology interaction
1546 airborne field investigations: Using lessons learned from the U.S. West coast in the design
1547 of activate off the U.S. East Coast, Bull. Am. Meteorol. Soc., 100(8), 1511–1528,
1548 <https://doi.org/10.1175/BAMS-D-18-0100.1>, 2019.

1549 Sorooshian, A., Corral, A. F., Braun, R. A., Cairns, B., Crosbie, E., Ferrare, R., Hair, J., Kleb, M.
1550 M., Hossein Mardi, A., Maring, H., McComiskey, A., Moore, R., Painemal, D., Scarino,
1551 A. J., Schlosser, J., Shingler, T., Shook, M., Wang, H., Zeng, X., Ziemba, L. and Zuidema,
1552 P.: Atmospheric Research Over the Western North Atlantic Ocean Region and North
1553 American East Coast: A Review of Past Work and Challenges Ahead, J. Geophys. Res.
1554 Atmos., in press, <https://doi.org/10.1029/2019JD031626>, 2020.

1555 Strapp, J. W., Leaitch, W. R. and Liu, P. S. K.: Hydrated and dried aerosol-size-distribution
1556 measurements from the Particle Measuring Systems FSSP-300 probe and the deiced

1557 PCASP-100X probe, *J. Atmos. Ocean. Technol.*, 9(5), 548–555,
 1558 [https://doi.org/10.1175/1520-0426\(1992\)009<0548:HADASD>2.0.CO;2](https://doi.org/10.1175/1520-0426(1992)009<0548:HADASD>2.0.CO;2), 1992.
 1559 Twomey, S.: The nuclei of natural cloud formation part II: The supersaturation in natural clouds
 1560 and the variation of cloud droplet concentration, *Geophys. Pura e Appl.*, 43(1), 243–249,
 1561 <https://doi.org/10.1007/BF01993560>, 1959.
 1562 Twomey, S.: The influence of pollution on the shortwave albedo of clouds, *J. Atmos. Sci.*, 34,
 1563 1149–1152, [https://doi.org/10.1175/1520-0469\(1977\)034<1149:TIOPOT>2.0.CO;2](https://doi.org/10.1175/1520-0469(1977)034<1149:TIOPOT>2.0.CO;2), 1977.
 1564 Van Dingenen, R., Raes, F. and Jensen, N. R.: Evidence for anthropogenic impact on number
 1565 concentration and sulfate content of cloud-processed aerosol particles over the North
 1566 Atlantic, *J. Geophys. Res. Atmos.*, 100(D10), 21057–21067,
 1567 <https://doi.org/10.1029/95jd02141>, 1995.
 1568 Wang, Z., Sorooshian, A., Prabhakar, G., Coggon, M. M. and Jonsson, H. H.: Impact of
 1569 emissions from shipping, land, and the ocean on stratocumulus cloud water elemental
 1570 composition during the 2011 E-PEACE field campaign, *Atmos. Environ.*, 89, 570–580,
 1571 <https://doi.org/10.1016/j.atmosenv.2014.01.020>, 2014.
 1572 Wang, Z., Mora Ramirez, M., Dadashazar, H., MacDonald, A. B., Crosbie, E., Bates, K. H.,
 1573 Coggon, M. M., Craven, J. S., Lynch, P., Campbell, J. R., Azadi Aghdam, M., Woods, R.
 1574 K., Jonsson, H., Flagan, R. C., Seinfeld, J. H. and Sorooshian, A.: Contrasting cloud
 1575 composition between coupled and decoupled marine boundary layer clouds, *J. Geophys.*
 1576 *Res. Atmos.*, 121(19), 11679–11691, <https://doi.org/10.1002/2016JD025695>, 2016.
 1577 West, R. E. L., Stier, P., Jones, A., Johnson, C. E., Mann, G. W., Bellouin, N., Partridge, D. G.
 1578 and Kipling, Z.: The importance of vertical velocity variability for estimates of the
 1579 indirect aerosol effects, *Atmos. Chem. Phys.*, 14(12), 6369–6393,
 1580 <https://doi.org/10.5194/acp-14-6369-2014>, 2014.
 1581 Wonaschütz, A., Coggon, M., Sorooshian, A., Modini, R., Frossard, A. A., Ahlm, L.,
 1582 Müllmenstädt, J., Roberts, G. C., Russell, L. M., Dey, S., Brechtel, F. J. and Seinfeld, J. H.:
 1583 Hygroscopic properties of smoke-generated organic aerosol particles emitted in the marine
 1584 atmosphere, *Atmos. Chem. Phys.*, 13(19), 9819–9835, [https://doi.org/10.5194/acp-13-](https://doi.org/10.5194/acp-13-9819-2013)
 1585 [9819-2013](https://doi.org/10.5194/acp-13-9819-2013), 2013.
 1586 Xue, H. and Feingold, G.: A modeling study of the effect of nitric acid on cloud properties, *J.*
 1587 *Geophys. Res.*, 109, D18204, <https://doi.org/10.1029/2004JD004750>, 2004.
 1588
 1589

1590 **Table 1.** Summary of field campaign data sets used in this study and statistics related to cloud
 1591 water sample collection. Smoke-influenced RFs were NiCE RFs 16–23 and FASE RFs 3–
 1592 11 and 13–15.

Field campaign	Dates (mm/dd/yyyy)	# of RFs	# of samples	# of fire-impacted samples
Eastern Pacific Emitted Aerosol Cloud Experiment (E-PEACE)	07/08/2011 – 08/18/2011	30	82	0
Nucleation in California Experiment (NiCE)	07/08/2013 – 08/07/2013	23	119	31
Biological and Oceanic Atmospheric Study (BOAS)	07/02/2015 – 07/24/2015	15	29	0
Fog and Stratocumulus Evolution Experiment (FASE)	07/18/2016 – 08/12/2016	16	155	136

1593
 1594
 1595
 1596

<u>Field campaign</u>	<u>Dates (mm/dd/yyyy)</u>	<u># of RFs</u>	<u># of samples</u>	<u># of fire-impacted samples</u>
<u>Eastern Pacific Emitted Aerosol Cloud Experiment (E-PEACE)</u>	<u>07/08/2011 – 08/18/2011</u>	<u>30</u>	<u>82</u>	<u>0</u>
<u>Nucleation in California Experiment (NiCE)</u>	<u>07/08/2013 – 08/07/2013</u>	<u>23</u>	<u>119</u>	<u>31</u>
<u>Biological and Oceanic Atmospheric Study (BOAS)</u>	<u>07/02/2015 – 07/24/2015</u>	<u>15</u>	<u>29</u>	<u>0</u>
<u>Fog and Stratocumulus Evolution Experiment (FASE)</u>	<u>07/18/2016 – 08/12/2016</u>	<u>16</u>	<u>155</u>	<u>136</u>

1597

1598 **Table 2.** Summary of chemical species analyzed in this study. IC = ion chromatography; ICP =
 1599 ICP-MS or ICP-QQQ. Note: NSS species, with the exception of NSS-SO₄²⁻, were calculated
 1600 using elements, not ions, hence they have no superscript charge.

Elements (ICP)		Inorganic ions (IC)	Organic ions (IC)
1 Ag	24 Na	47 Ammonium (NH ₄ ⁺)	66 Acetate
2 Al	25 Nb	48 Bromide (Br ⁻)	67 Adipate
3 As	26 Ni	49 Calcium (Ca ²⁺)	68 Butyrate
4 B	27 P	50 Chloride (Cl ⁻)	69 Formate
5 Ba	28 Pb	51 Fluoride (F ⁻)	70 Glutarate
6 Br	29 Pd	52 Lithium (Li ⁺)	71 Glycolate
7 C	30 Rb	53 Magnesium (Mg ²⁺)	72 Glyoxylate
8 Ca	31 Rh	54 Methanesulfonic acid (MSA)	73 Lactate
9 Cd	32 Ru	55 Nitrate (NO ₃ ⁻)	74 Maleate
10 Cl	33 S	56 Nitrite (NO ₂ ⁻)	75 Malonate
11 Co	34 Sb	57 Potassium (K ⁺)	76 Oxalate
12 Cr	35 Se	58 Sodium (Na ⁺)	77 Propionate
13 Cs	36 Si	59 Sulfate (SO ₄ ²⁻)	78 Pyruvate
14 Cu	37 Sn		79 Succinate
15 Fe	38 Sr	<u>Amines (IC)</u>	
16 Ga	39 Ta	60 Diethyl ammonium (DEA)	
17 Hf	40 Te	61 Dimethyl ammonium (DMA)	
18 I	41 Ti		
19 K	42 V	<u>NSS species (calculated)</u>	
20 Li	43 W	62 NSS Calcium (NSS-Ca)	
21 Mg	44 Y	63 NSS Potassium (NSS-K)	
22 Mn	45 Zn	64 NSS Magnesium (NSS-Mg)	
23 Mo	46 Zr	65 NSS Sulfate (NSS-SO ₄ ²⁻)	

1601
 1602
 1603
 1604
 1605

Elements (ICP)		Inorganic ions (IC)	Organic ions (IC)
1 Ag	24 Na	47 Ammonium (NH ₄ ⁺)	66 Acetate
2 Al	25 Nb	48 Bromide (Br ⁻)	67 Adipate
3 As	26 Ni	49 Calcium (Ca ²⁺)	68 Butyrate
4 B	27 P	50 Chloride (Cl ⁻)	69 Formate
5 Ba	28 Pb	51 Fluoride (F ⁻)	70 Glutarate
6 Br	29 Pd	52 Lithium (Li ⁺)	71 Glycolate
7 C	30 Rb	53 Magnesium (Mg ²⁺)	72 Glyoxylate
8 Ca	31 Rh	54 Methanesulfonic acid (MSA)	73 Lactate

<u>9</u>	<u>Cd</u>	<u>32</u>	<u>Ru</u>	<u>55</u>	<u>Nitrate (NO₃⁻)</u>	<u>74</u>	<u>Maleate</u>
<u>10</u>	<u>Cl</u>	<u>33</u>	<u>S</u>	<u>56</u>	<u>Nitrite (NO₂⁻)</u>	<u>75</u>	<u>Malonate</u>
<u>11</u>	<u>Co</u>	<u>34</u>	<u>Sb</u>	<u>57</u>	<u>Potassium (K⁺)</u>	<u>76</u>	<u>Oxalate</u>
<u>12</u>	<u>Cr</u>	<u>35</u>	<u>Se</u>	<u>58</u>	<u>Sodium (Na⁺)</u>	<u>77</u>	<u>Propionate</u>
<u>13</u>	<u>Cs</u>	<u>36</u>	<u>Si</u>	<u>59</u>	<u>Sulfate (SO₄²⁻)</u>	<u>78</u>	<u>Pyruvate</u>
<u>14</u>	<u>Cu</u>	<u>37</u>	<u>Sn</u>			<u>79</u>	<u>Succinate</u>
<u>15</u>	<u>Fe</u>	<u>38</u>	<u>Sr</u>		<u>Amines (IC)</u>		
<u>16</u>	<u>Ga</u>	<u>39</u>	<u>Ta</u>	<u>60</u>	<u>Diethylamine (DEA)</u>		<u>Acidity (pH)</u>
<u>17</u>	<u>Hf</u>	<u>40</u>	<u>Te</u>	<u>61</u>	<u>Dimethylamine (DMA)</u>	<u>80</u>	<u>Hydrogen ion (H⁺)</u>
<u>18</u>	<u>I</u>	<u>41</u>	<u>Ti</u>				
<u>19</u>	<u>K</u>	<u>42</u>	<u>V</u>		<u>NSS species (calculated)</u>		
<u>20</u>	<u>Li</u>	<u>43</u>	<u>W</u>	<u>62</u>	<u>NSS Calcium (NSS-Ca)</u>		
<u>21</u>	<u>Mg</u>	<u>44</u>	<u>Y</u>	<u>63</u>	<u>NSS Potassium (NSS-K)</u>		
<u>22</u>	<u>Mn</u>	<u>45</u>	<u>Zn</u>	<u>64</u>	<u>NSS Magnesium (NSS-Mg)</u>		
<u>23</u>	<u>Mo</u>	<u>46</u>	<u>Zr</u>	<u>65</u>	<u>NSS Sulfate (NSS-SO₄²⁻)</u>		

1606

1607 **Table 3.** Summary of one-predictor models for N_d based on using any of nine of the final
 1608 chemical species that were identified after applying the filtering scheme shown in Figure 2. The
 1609 coefficients correspond to a linear model of the form $\log(N_d) = a_0 + a_1 \log(M_i)$, where M_i is the
 1610 mass concentration of species i .

Species	R^2_{adj}	Coefficients	
		a_0	a_1
Tot-SO ₄ ²⁻	0.40	2.05	0.32
NH ₄ ⁺	0.34	2.33	0.25
NSS-SO ₄ ²⁻	0.29	2.13	0.28
MSA	0.26	2.37	0.31
NO ₃ ⁻	0.24	2.12	0.25
Na	0.19	2.03	0.13
Ox	0.15	2.26	0.18
V	0.14	2.61	0.15
Fe	0.05	2.26	0.09

Formatted: Font: Italic

Formatted: Font: Italic

Formatted: Font: Italic

Formatted: Font: Italic

1611

Species	R^2_{adj}	Coefficients	
		a_0	a_1
Tot-SO ₄ ²⁻	0.40	2.05	0.32
NH ₄ ⁺	0.34	2.33	0.25
NSS-SO ₄ ²⁻	0.29	2.13	0.28
MSA	0.26	2.37	0.31
NO ₃ ⁻	0.24	2.12	0.25
Na	0.19	2.03	0.13
Ox	0.15	2.26	0.18
V	0.14	2.61	0.15
Fe	0.05	2.26	0.09

1612

1613 **Table 4.** Comparison of coefficient values for studies that correlate N_d to SO_4^{2-} (total or non-sea
 1614 salt). The coefficients correspond to a linear model of the form $\log(N_d) = a_0 + a_1 \log(SO_4^{2-})$.

Reference	a_0	a_1	SO_4^{2-}	R^2	Cloud type
Leaitch et al. (1992) ^a	1.95	0.257	Tot	0.3	Stratocumulus
	2.33	0.186	Tot	0.49	Cumulus
Novakov et al. (1994)	2.323	0.091	NSS	0.50 ^b	Marine stratocumulus
	2.43	-0.056	NSS	0.03	Marine cumulus
Van Dingenen et al. (1995) ^c	2.33	0.4	NSS	0.42	All cloud types combined
	2.24	0.257	NSS	^d	Continental stratus
Boucher & Lohmann (1995) ^c	2.54	0.186	NSS	^d	Continental cumulus
	2.06	0.48	NSS	^d	Marine
	2.21	0.41	NSS	^d	All cloud types combined
Saxena & Menon (1999)	0.67	0.66	Tot	^d	Continental orographic clouds
	2.32	0.74	NSS	0.82	Marine
Lowenthal et al. (2004)	2.38	0.49	NSS	0.66	Continental
	2.39	0.5	NSS	0.81	Combined
McCoy et al. (2017)	2.11	0.41	NSS	0.36	Marine stratocumulus

^a The units of SO_4^{2-} for this regression are $nEq\ m^{-3}$. All other studies report SO_4^{2-} in units of $\mu g\ m^{-3}$.

However, the value of a_1 is not affected by the units of concentration.

^b The R^2 has a $p > 0.05$ due to having few data points.

^c These regressions were made using data compiled from several studies and assume that $N_{CCN} \sim N_d$.

^d Study does not report R^2 .

Formatted: Font: Italic

Formatted: Font: Italic

Formatted: Font: Italic

1615
1616

Reference	a_0	a_1	SO_4^{2-}	R^2	Cloud type
Leaitch et al. (1992) ^a	1.95	0.257	Tot	0.3	Continental stratocumulus
	2.33	0.186	Tot	0.49	Continental cumulus
Novakov et al. (1994)	2.323	0.091	NSS	0.50 ^b	Marine stratocumulus
	2.43	-0.056	NSS	0.03	Marine cumulus
Van Dingenen et al. (1995) ^c	2.33	0.4	NSS	0.42	All cloud types combined
	2.24	0.257	NSS	^d	Continental stratus
Boucher & Lohmann (1995) ^c	2.54	0.186	NSS	^d	Continental cumulus
	2.06	0.48	NSS	^d	Marine
	2.21	0.41	NSS	^d	All cloud types combined
Saxena & Menon (1999)	0.67	0.66	Tot	^d	Continental orographic clouds
	2.32	0.74	NSS	0.82	Marine
Lowenthal et al. (2004)	2.38	0.49	NSS	0.66	Continental
	2.39	0.5	NSS	0.81	Combined

McCoy et al. (2017) 2.11 0.41 NSS 0.36 Marine stratocumulus

^a The units of SO_4^{2-} for this regression are nEq m^{-3} . All other studies report SO_4^{2-} in units of $\mu\text{g m}^{-3}$.
However, the value of the slope (a_j) is not affected by the units of concentration.

^b The R^2 has a $p > 0.05$ due to having few data points.

^c These regressions were made using data compiled from several studies and assume that $N_{CCN} \sim N_d$.

^d Study does not report R^2 .

1617

1618 **Table 5.** The top three statistically significant regressions with the highest R^2_{adj} for a given
 1619 number of predictors. The coefficients correspond to a linear model of the form $\log(N_{id}) = a_0 + \sum$
 1620 $a_i \log(P_i)$.
 1621

Formatted: Font: Italic

Formatted: Font: Italic

Formatted: Font: Italic

Formatted: Font: Italic

Formatted: Font: Not Bold

# of Predictors	Predictors (P_i) and their respective coefficients (a_i)											R^2_{adj}
	a_0	a_1	P_1	a_2	P_2	a_3	P_3	a_4	P_4	a_5	P_5	
1	2.05	0.32	Tot-SO ₄ ²⁻									0.40
	2.33	0.25	NH ₄ ⁺									0.34
	2.13	0.28	NSS-SO ₄ ²⁻									0.29
2	2.18	0.22	Tot-SO ₄ ²⁻	0.12	NH ₄ ⁺							0.48
	2.43	0.21	MSA	0.15	NH ₄ ⁺							0.44
	2.25	0.19	NH ₄ ⁺	0.09	Na							0.42
3	2.25	0.13	NSS-SO ₄ ²⁻	0.13	NH ₄ ⁺	0.10	Na					0.50
	2.24	0.19	Tot-SO ₄ ²⁻	0.10	Ox	0.07	NH ₄ ⁺					0.49
	2.25	0.17	Tot-SO ₄ ²⁻	0.11	NH ₄ ⁺	0.08	MSA					0.49
4	2.32	0.21	Tot-SO ₄ ²⁻	0.20	Ox	0.09	NH ₄ ⁺	-0.15	NO ₃ ⁻			0.52
	2.29	0.11	NSS-SO ₄ ²⁻	0.10	Ox	0.09	Na	0.08	NH ₄ ⁺			0.51
	2.31	0.11	NH ₄ ⁺	0.10	NSS	0.10	MSA	0.08	Na			0.51
5	2.10	0.13	Na	0.12	Ox	0.11	NSS-SO ₄ ²⁻	0.08	NH ₄ ⁺	-0.05	V	0.56
	2.40	0.23	Ox	0.13	NSS-SO ₄ ²⁻	0.10	NH ₄ ⁺	0.09	Na	-0.17	NO ₃ ⁻	0.55
	2.36	0.14	NH ₄ ⁺	0.14	MSA	0.12	NSS-SO ₄ ²⁻	0.07	Na	-0.08	NO ₃ ⁻	0.52

# of Predictors	Predictors (P_i) and their respective coefficients (a_i)											R^2_{adj}
	a_0	a_1	P_1	a_2	P_2	a_3	P_3	a_4	P_4	a_5	P_5	
1	2.05	0.32	Tot-SO ₄ ²⁻									0.40
	2.33	0.25	NH ₄ ⁺									0.34
	2.13	0.28	NSS-SO ₄ ²⁻									0.29
2	2.18	0.22	Tot-SO ₄ ²⁻	0.12	NH ₄ ⁺							0.48
	2.43	0.21	MSA	0.15	NH ₄ ⁺							0.44
	2.25	0.19	NH ₄ ⁺	0.09	Na							0.42
3	2.25	0.13	NSS-SO ₄ ²⁻	0.13	NH ₄ ⁺	0.10	Na					0.50
	2.24	0.19	Tot-SO ₄ ²⁻	0.10	Ox	0.07	NH ₄ ⁺					0.49
	2.25	0.17	Tot-SO ₄ ²⁻	0.11	NH ₄ ⁺	0.08	MSA					0.49
4	2.32	0.21	Tot-SO ₄ ²⁻	0.20	Ox	0.09	NH ₄ ⁺	0.15	NO ₃ ⁻			0.52
	2.29	0.11	NSS-SO ₄ ²⁻	0.10	Ox	0.09	Na	0.08	NH ₄ ⁺			0.51
	2.31	0.11	NH ₄ ⁺	0.10	NSS	0.10	MSA	0.08	Na			0.51
5	2.10	0.13	Na	0.12	Ox	0.11	NSS-SO ₄ ²⁻	0.08	NH ₄ ⁺	-0.05	V	0.56
	2.40	0.23	Ox	0.13	NSS-SO ₄ ²⁻	0.10	NH ₄ ⁺	0.09	Na	-0.17	NO ₃ ⁻	0.55
	2.36	0.14	NH ₄ ⁺	0.14	MSA	0.12	NSS-SO ₄ ²⁻	0.07	Na	-0.08	NO ₃ ⁻	0.52

1623

1624 **Table 6.** Comparison of regressions containing NSS-SO_4^{2-} , Na, and Ox.

# of Predictors	Predictors (P_i) and their respective coefficients (a_i)							R^2_{adj}
	a_0	a_1	P_1	a_2	P_2	a_3	P_3	
1	2.13	0.28	NSS-SO_4^{2-}					0.29
2	2.12	0.23	NSS-SO_4^{2-}	0.12	Na			0.40
	2.26	0.24	NSS-SO_4^{2-}	0.12	Ox			0.34
3	2.22	0.22	NSS-SO_4^{2-}	0.10	Na	0.08	Ox	0.42

# of Predictors	Predictors (P_i) and their respective coefficients (a_i)							R^2_{adj}
	a_0	a_1	P_1	a_2	P_2	a_3	P_3	
1	2.13	0.28	NSS-SO_4^{2-}	-	-	-	-	0.29
2	2.12	0.23	NSS-SO_4^{2-}	0.12	Na			0.40
	2.26	0.24	NSS-SO_4^{2-}	0.12	Ox	-	-	0.34
3	2.22	0.22	NSS-SO_4^{2-}	0.10	Na	0.08	Ox	0.42

1629 **Table 7.** Results of multivariable regressions from previous studies that have correlated N_d to
 1630 mass concentrations. The regression corresponds to a model like Equation 3. OM = Organic
 1631 Matter, SS = Sea Salt, BC = Black Carbon, DU = Dust.

Reference	Predictors (P_i) and their respective coefficients (a_i)										R^2	Cloud type
	a_0	a_1	P_1	a_2	P_2	a_3	P_3	a_4	P_4			
Menon et al. (2002) ^a	2.41	0.50	NSS-SO ₄ ²⁻	0.13	OM ^b							Continental
	2.41	0.50	NSS-SO ₄ ²⁻	0.13	OM	0.05	SS					Marine
McCoy et al. (2017)	1.78	0.31	NSS-SO ₄ ²⁻	-0.19	SS	0.057	BC	0.031	DU	0.44		Marine stratocumulus (global average)
McCoy et al. (2018)	2.03	0.2	NSS-SO ₄ ²⁻	-0.04	SS	-0.03	BC	0	DU	0.08		Marine stratocumulus (just Californian coast)

^a This study obtains data from other studies and calculates organic matter.

^b OM = Organic Matter, SS = Sea Salt, BC = Black Carbon, DU = Dust.

Reference	Predictors (P_i) and their respective coefficients (a_i)										R^2	Cloud type
	a_0	a_1	P_1	a_2	P_2	a_3	P_3	a_4	P_4			
Menon et al. (2002) ^a	2.41	0.50	NSS-SO ₄ ²⁻	0.13	OM							Continental
	2.41	0.50	NSS-SO ₄ ²⁻	0.13	OM	0.05	SS					Marine
McCoy et al. (2017)	1.78	0.31	NSS-SO ₄ ²⁻	-0.19	SS	0.057	BC	0.031	DU	0.44		Marine stratocumulus (global average)
McCoy et al. (2018)	2.03	0.2	NSS-SO ₄ ²⁻	-0.04	SS	-0.03	BC	0	DU	0.08		Marine stratocumulus (just Californian coast)

^a This study obtains data from other studies and calculates organic matter.

1632
1633
1634

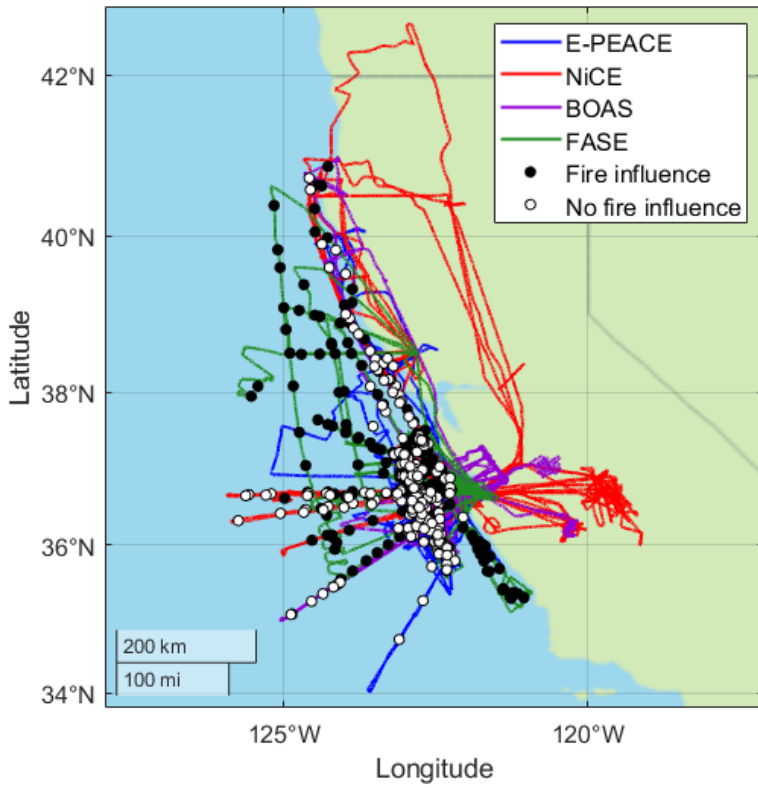
1635

1636 **Table 8.** Summary of the R^2_{adj} obtained when correlating mass concentration of a species to N_d
 1637 under different atmospheric conditions.

Binning criterion	Data points considered	R^2_{adj}			
		NSS-SO ₄ ²⁻	Na	Ox	Fe
None	All	0.29	0.19	0.15	0.05
Turbulence	High σ_w	0.27	0.26	0.09	0.02 ^a
	Low σ_w	0.27	0.09	0.30	0.07
Smoke influence	Smoke	0.22	0.17	0.42	0.15
	No smoke	0.36	0.24	0.07	0.04
Normalized cloud height	Top third	0.33	0.33	0.08	0.03
	Middle third	0.29	0.16	0.16	0.03
	Bottom third	0.17	0.10	0.29	0.20

^a This R^2_{adj} has a p-value > 0.05.

1638
 1639
 1640
 1641
 1642

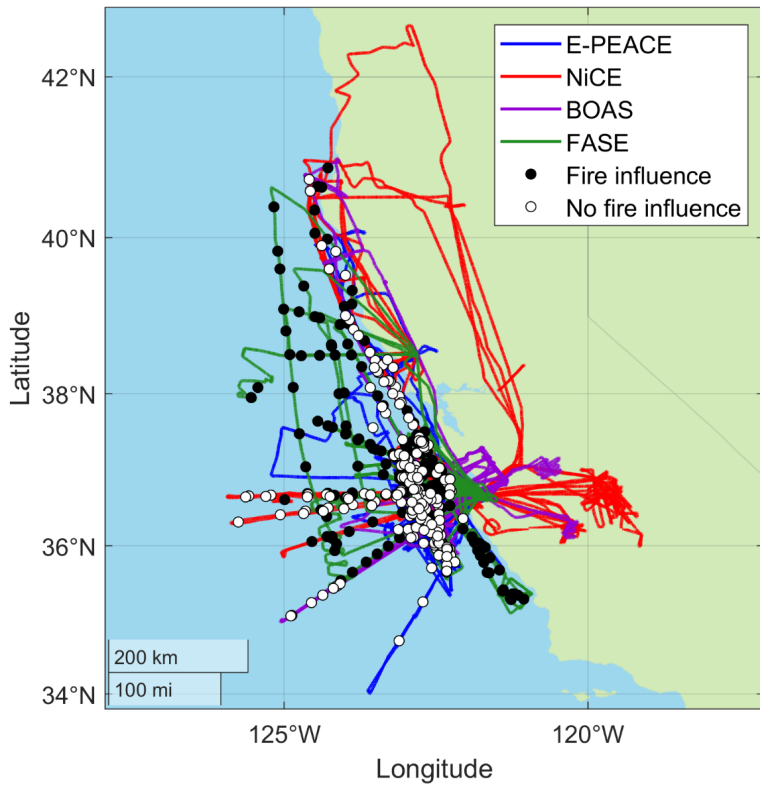


1643
1644

Binning criterion	Data points considered	R^2_{adi}			
		NSS-SO ₄ ²⁻	Na	Ox	Fe
None	All	0.29	0.19	0.15	0.05
Turbulence	High σ_w	0.27	0.26	0.09	0.02 ^a
	Low σ_w	0.27	0.09	0.30	0.07
Smoke influence	No smoke	0.36	0.24	0.07	0.04
	Smoke	0.22	0.17	0.42	0.15
	NiCE ^b	0.36	0.46	0.60	0.28
	FASE ^b	0.18	0.13	0.41	0.12
Normalized cloud height	Top third	0.33	0.33	0.08	0.03
	Middle third	0.29	0.16	0.16	0.03
	Bottom third	0.17	0.10	0.29	0.20

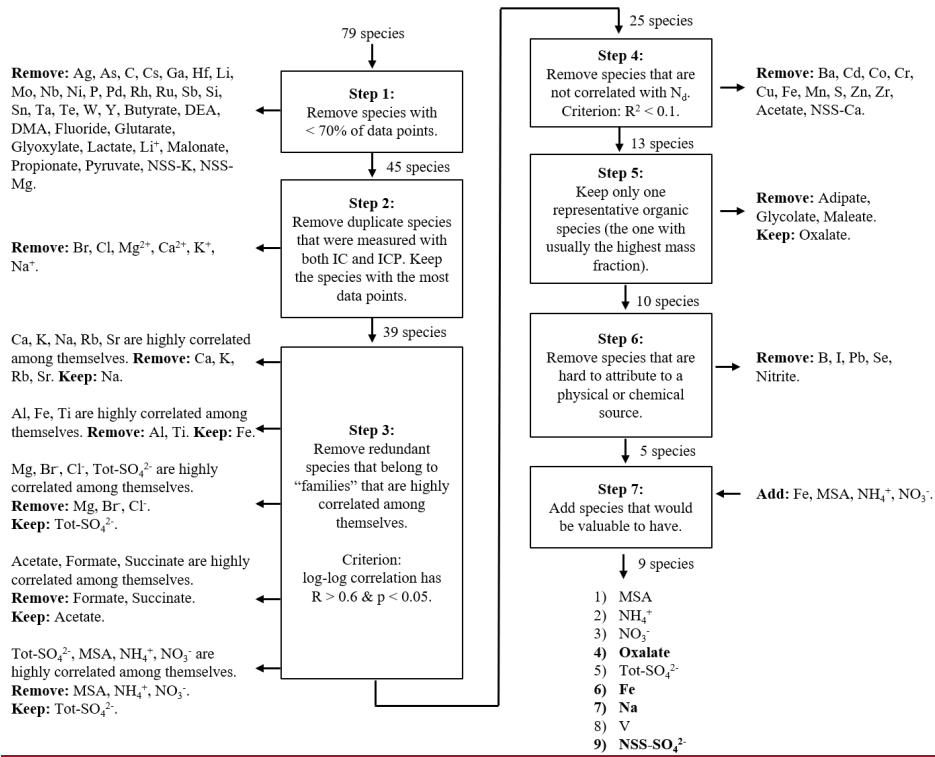
^a This R^2_{adj} has a p-value > 0.05 .

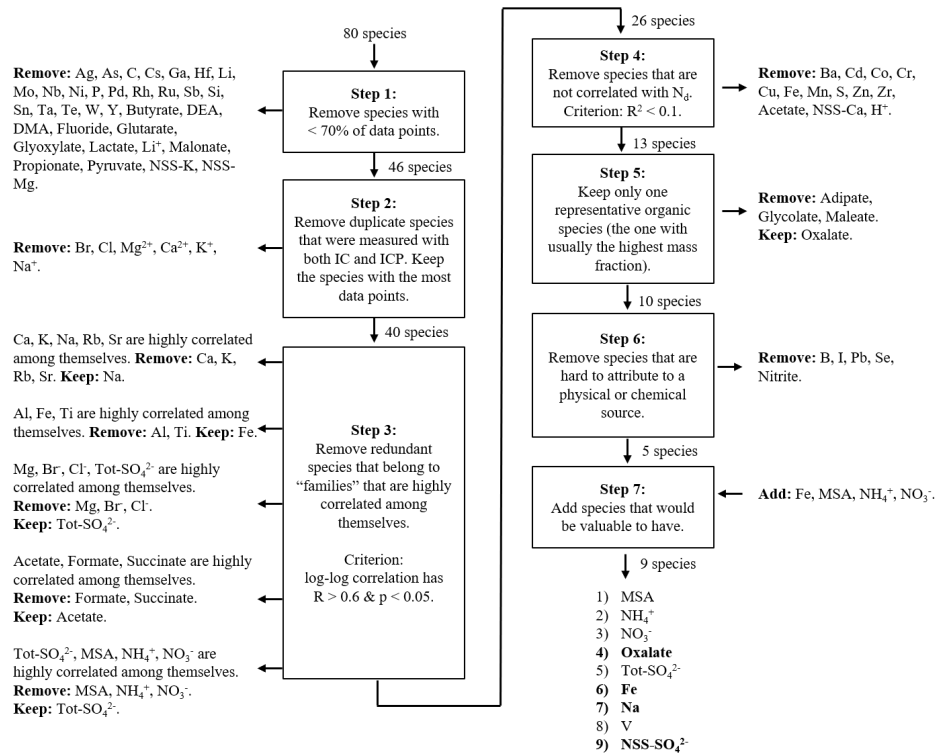
^b Only smoke-influenced samples in this campaign were considered.



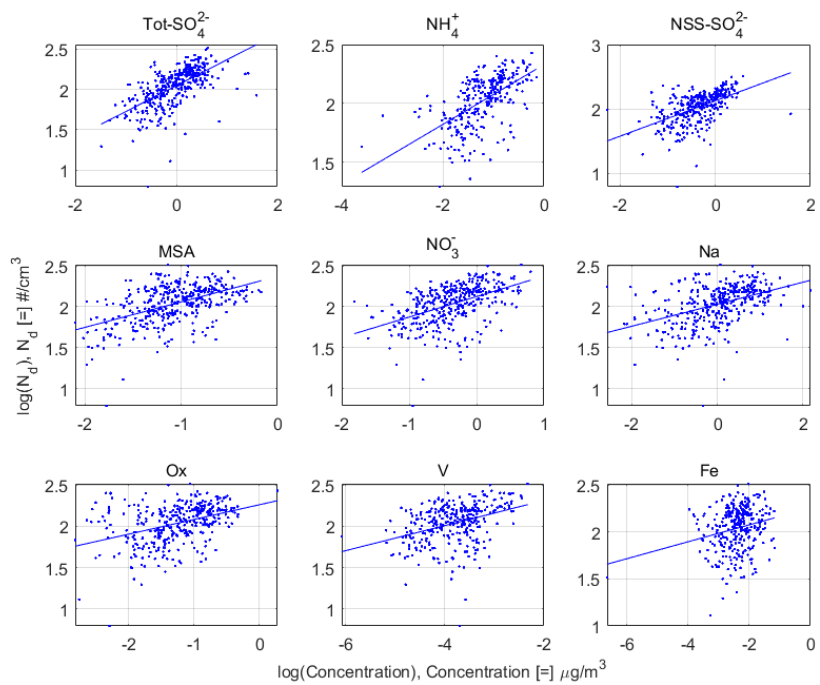
1646
 1647 **Figure 1.** Flight paths for each of the four campaigns used in this study. Markers indicate the
 1648 average location at which the cloud water samples were collected. Smoke- and non-smoke-
 1649 influenced samples are indicated with filled and open markers, respectively.

1650
 1651
 1652

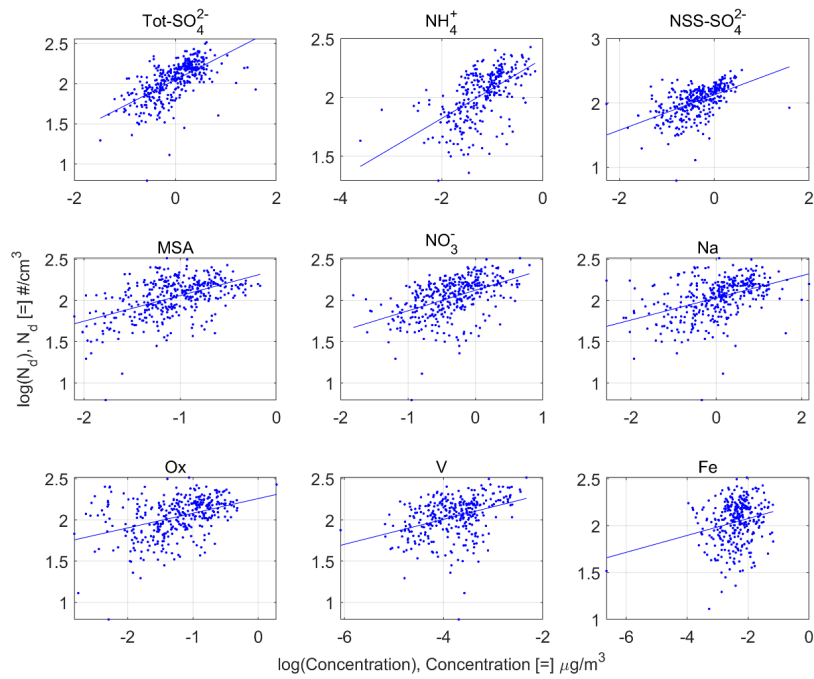




1655
 1656 **Figure 2.** Algorithm used to filter the number of species from 7980 to 9. The four bolded species
 1657 are the ones used in Section 3.3). ICP = ICP-MS + ICP-QQQ.
 1658
 1659
 1660



1661
1662



1663
 1664 **Figure 3.** Scatter plot for the nine filtered species from Figure 2. The lines are linear regression
 1665 models of the form $\log(N_d) = a_0 + a_1 \log(M_i)$, where M_i is the mass concentration of species i .
 1666
 1667

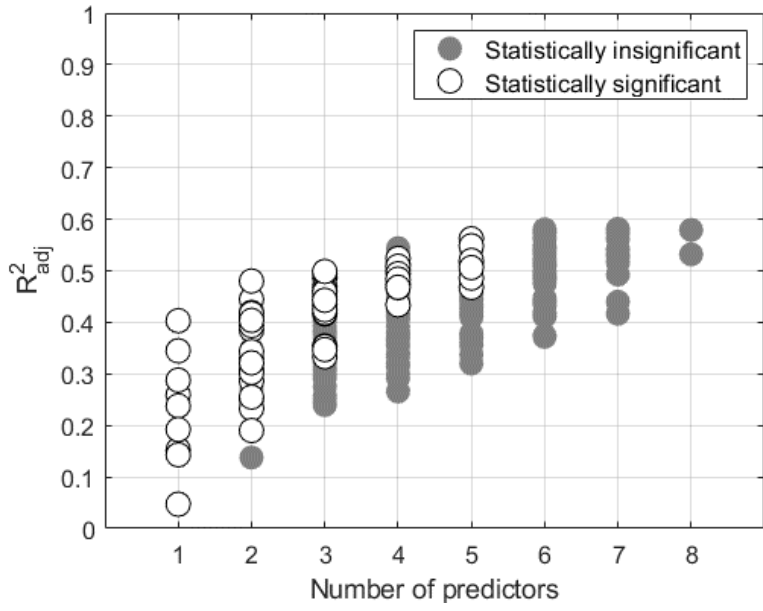
Formatted: Font: Italic

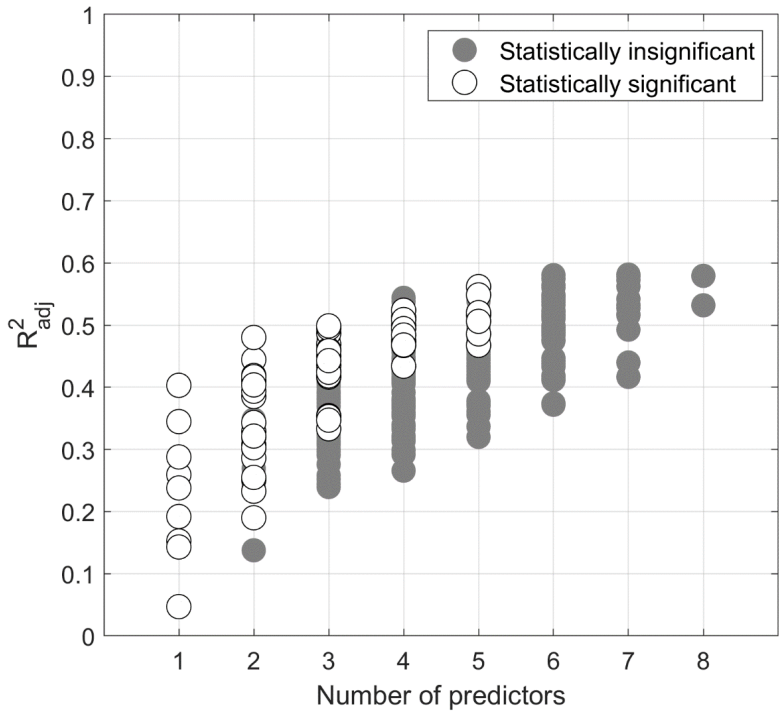
Formatted: Font: Italic

Formatted: Font: Italic

Formatted: Font: Italic

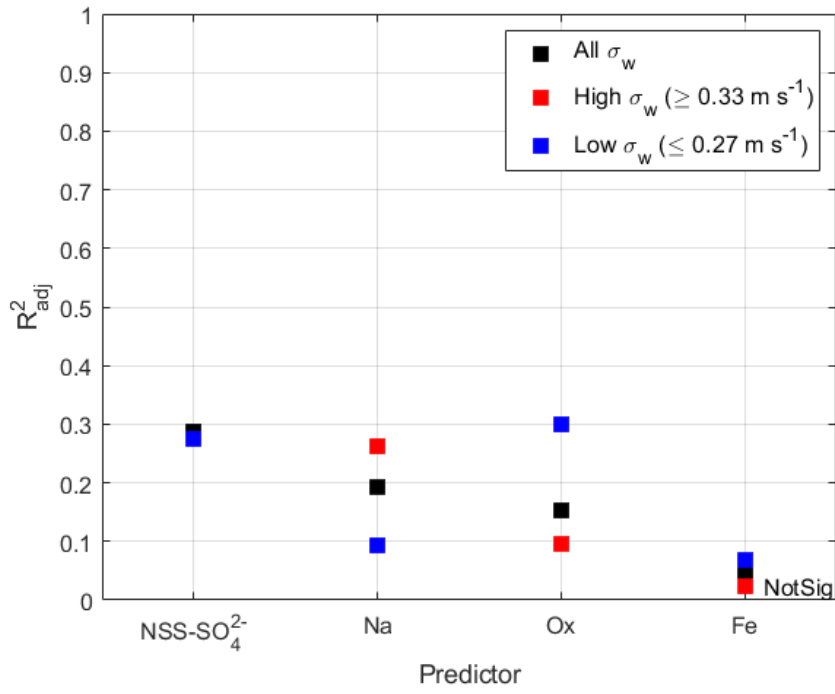
1668
1669



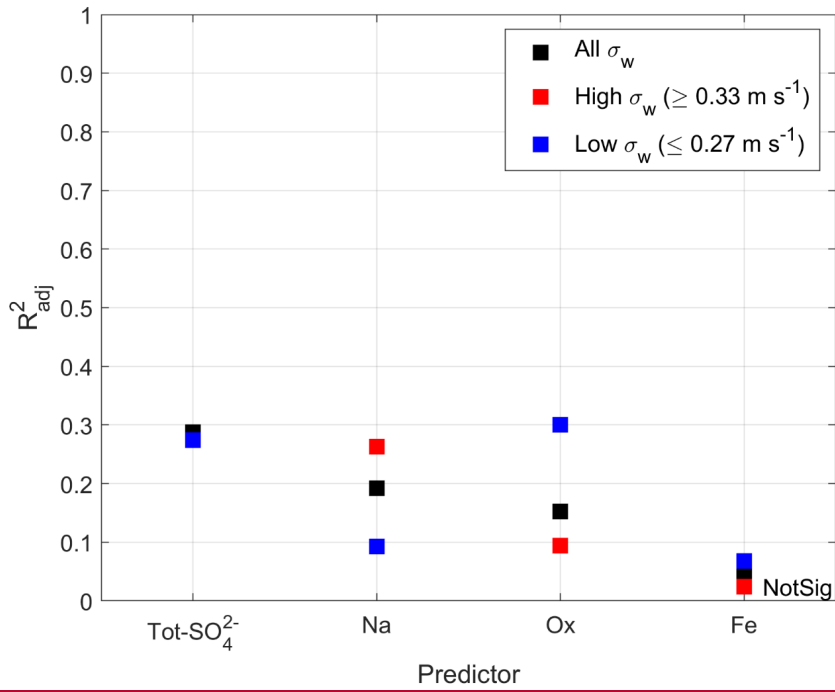


1670
 1671
 1672
 1673
 1674
 1675

Figure 4. Plot showing which of the 383 regressions are statistically significant. This plot ignores the regressions that use both NSS-SO₄²⁻ and Tot-SO₄²⁻ simultaneously.

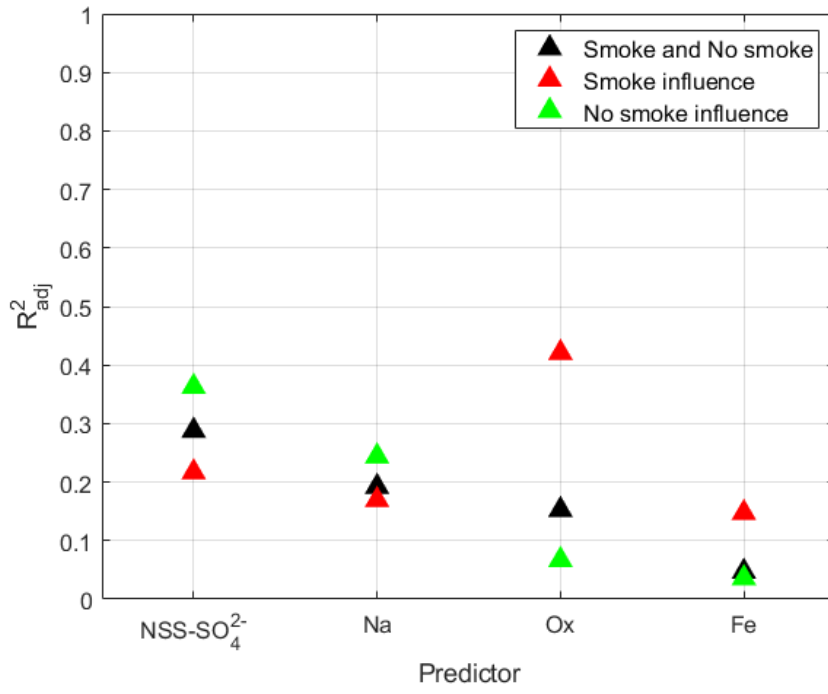


1676
1677

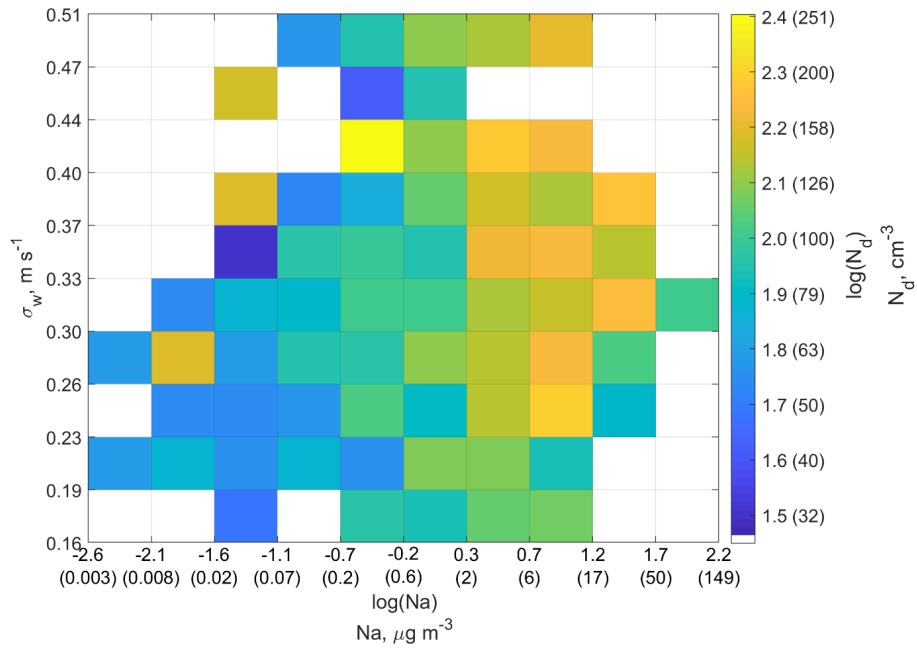


1678
 1679 **Figure 5.** Effect of turbulence (quantified using σ_w) on the ability of a single species to predict
 1680 N_d . For NSS-SO₄²⁻, the high (red) and low (blue) σ_w data points overlap. NotSig = Not
 1681 statistically significant according to the definition in Section 2.5.

1682
 1683
 1684



1685
1686



1687
 1688 **Figure 6.** Heatmap showing the dependence of N_d on both σ_w and Na. The lower and upper
 1689 bounds for the x-axis, y-axis, and color bar cover the entire range of σ_w , Na, and N_d , respectively.
 1690 To assist in physical interpretation, the tick markings on the x-axis and color bar show two
 1691 numbers: those without parenthesis correspond to $\log(\text{Na})$ or $\log(N_d)$; those within parenthesis
 1692 correspond to Na or N_d , in their respective units.
 1693

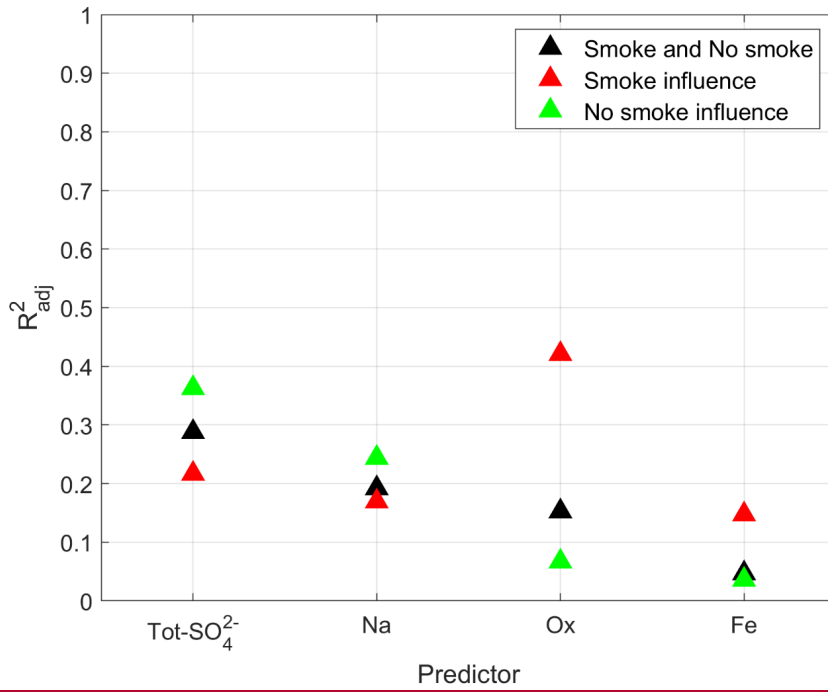
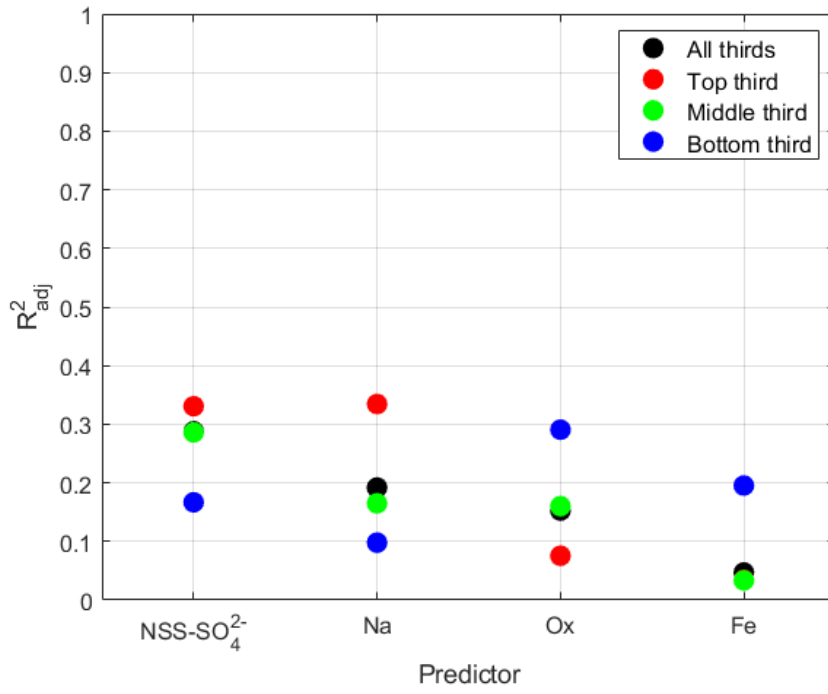
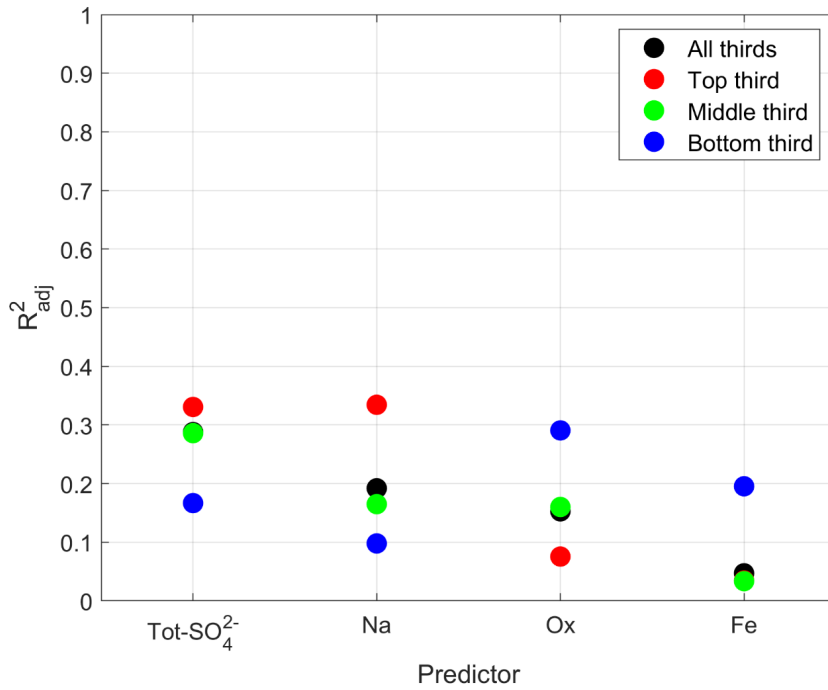


Figure 7. Effect of the influence of smoke on the ability of a single species to predict N_d .

1694
 1695
 1696
 1697
 1698

1699
1700





1701
 1702
 1703
 1704
 1705
 1706
 1707

Figure 78. Effect of the influence of normalized cloud height on the ability of a single species to predict N_d . For Fe, the top 3rd (red) data point overlaps with the middle and bottom 3rd (green and blue) data points.